AD___________________

Award Number: W81XWH-06-01-0791

TITLE: Development and Optimization of a Dedicated, Hybrid Dual-Modality SPECT-CmT System for Improved Breast Lesion Diagnosis

PRINCIPAL INVESTIGATOR: Priti Madhav

CONTRACTING ORGANIZATION: Duke University
Durham NC, 27710

REPORT DATE: January 2008

TYPE OF REPORT: Annual Summary

PREPARED FOR: U.S. Army Medical Research and Materiel Command
Fort Detrick, Maryland 21702-5012

REPORT DOCUMENTATION PAGE

Form Approved
OMB No. 0704-0188

1. REPORT DATE *(DD-MM-YYYY)*
01-01-2008

2. REPORT TYPE
Annual Summary

3. DATES COVERED *(From - To)*
31 JAN 2007 - 31 DEC 2007

4. TITLE AND SUBTITLE
Development and Optimization of a Dedicated, Hybrid Dual-Modality SPECT-CmT System for Improved Breast Lesion Diagnosis

5a. CONTRACT NUMBER

5b. GRANT NUMBER
W81XWH-06-01-0791

5c. PROGRAM ELEMENT NUMBER

6. AUTHOR(S)
Priti Madhav

E-Mail: priti.madhav@duke.edu

5d. PROJECT NUMBER

5e. TASK NUMBER

5f. WORK UNIT NUMBER

7. PERFORMING ORGANIZATION NAME(S) AND ADDRESS(ES)
Duke University
Durham NC, 27710

8. PERFORMING ORGANIZATION REPORT NUMBER

9. SPONSORING / MONITORING AGENCY NAME(S) AND ADDRESS(ES)
U.S. Army Medical Research and Materiel Command
Fort Detrick, Maryland 21702-5012

10. SPONSOR/MONITOR'S ACRONYM(S)

11. SPONSOR/MONITOR'S REPORT NUMBER(S)

12. DISTRIBUTION / AVAILABILITY STATEMENT
Approved for Public Release; Distribution Unlimited

13. SUPPLEMENTARY NOTES

14. ABSTRACT
The overall objective of this project is to implement a dual-modality single photon emission computed tomography (SPECT) and x-ray computed mammotomography (CmT) system for the detection and staging of breast cancer, monitoring of treatment therapies, and improving surgical biopsy guidance. The sequential acquisition with emission (nuclear) and transmission (x-ray) 3D imaging systems can aid in localizing the radioactive uptake of a tumor from the emission image by using the anatomical structure from the transmission image. In the first year, both systems were integrated onto a single platform with a customized patient bed to allow emission and transmission imaging of a pendant, uncompressed breast during a single session. Further investigation was done to ensure that each system was positioned such that it could fit over the patient bed and completely sample the breast. Physical constraints of each system were examined. A data acquisition sequence was designed for SPECT and CmT. Imaging feasibility with geometric phantoms and breast phantoms were performed to study the resolution/sampling properties and fusion of functional-anatomical images. One hybrid patient study was also carried out. In the next two years of this grant, corrections due to the CmT offset geometry, x-ray scatter, and attenuation will be applied to increase contrast, decrease noise, and improve quantitative accuracy in the images. In addition to research, clinical experience in other areas of breast cancer detection was explored.

15. SUBJECT TERMS
X-ray imaging, Nuclear Medicine Imaging, SPECT, CT, Molecular Breast Imaging, Mammotomography

16. SECURITY CLASSIFICATION OF: a. REPORT	b. ABSTRACT	c. THIS PAGE	17. LIMITATION OF ABSTRACT	18. NUMBER OF PAGES	19a. NAME OF RESPONSIBLE PERSON
U	U	U	UU	41	USAMRMC
					19b. TELEPHONE NUMBER *(include area code)*

Standard Form 298 (Rev. 8-98)
Prescribed by ANSI Std. Z39.18

Table of Contents

A. INTRODUCTION

The overall objective of this project is to implement a dual-modality single photon emission computed tomography (SPECT) and x-ray computed mammotomography (CmT) system for the detection and staging of breast cancer, monitoring of treatment therapies, and improving surgical biopsy guidance. The sequential acquisition with emission (nuclear) and transmission (x-ray) 3D imaging systems can aid in localizing the radioactive uptake of a tumor from the emission image by using the anatomical structure from the transmission image. In the first year, both systems were integrated onto a single platform with a customized patient bed to allow emission and transmission imaging of a pendant, uncompressed breast during a single session. Further investigation was done to ensure that each system was positioned such that it could fit over the patient bed and completely sample the breast. Physical constraints of each system were examined. A data acquisition sequence was designed for SPECT and CmT. Imaging feasibility with geometric phantoms and breast phantoms were performed to study the resolution/sampling properties and fusion of functional-anatomical images. One hybrid patient study was also carried out. In the next two years of this grant, corrections due to the CmT offset geometry, x-ray scatter, and attenuation will be applied to increase contrast, decrease noise, and improve quantitative accuracy in the images. In addition to research, clinical experience in other areas of breast cancer detection was explored.

B. BODY

Task 1: Design and implement a dual-modality prototype system

<u>*Task 1(d)*</u>

Although this task (as written in Appendix A, Statement of Works) was set out to be accomplished in the beginning of Year 2, it was necessary to first find the most possible optimal orientation of each of the sub-systems so that the dual-modality system could be built. In implementing a compact, dedicated SPECT-CmT hybrid system for breast imaging, the challenge was to place each of the sub-systems in an optimum orientation such that it would (1) provide suitable reconstructed images; (2) allow maximal access to the patient's breast; and (3) accommodate a custom patient bed that could fit above the compact hybrid system, shield the patient from scattered, low energy x-rays and photons, and maintain patient comfort. Previous cross-contamination results showed that the optimal placement was having the SPECT sub-system positioned 90° relative to the central x-ray axis [1, 2]. Unlike the SPECT sub-system, the CmT sub-system is restricted to a stationary polar tilt and can only rotate 360° around the vertical axis of a pendant breast in this initial hybrid prototype. However, in this orientation the CmT sub-system is limited in imaging deep into the breast and axillary region and closer to the chest wall, and introduces insufficient sampling which was previously shown to be overcome by using 3D complex acquisition trajectories [3]. Therefore a study was done to observe the effects of lesion distortion, geometric distortion, and sampling insufficiency on reconstructed images acquired with the CmT system at different stationary tilts and 3D complex acquisition trajectories [4]. A detailed description of this work and results was presented at the *2007 SPIE Medical Imaging Conference* for which I was the primary author. A conference proceeding was submitted and is attached in Appendix B.

This study was extended by taking a further look at sampling insufficiency at different tilts by acquiring images of a Defrise phantom (model ECT/MI-DEF/P, *Data Spectrum Corp.*, Hillsborough, NC) with 3.5mm diameter acrylic beads placed in between the gaps of each of the discs (Fig. 1, LEFT). More details on each of the acquisition trajectories can be found in Appendix B (Fig. 5). Figure 1 shows the sagittal reconstructed slices of the Defrise phantom for all acquisition trajectories. The tilted acquisition orbits show disc distortion, especially for ones acquired with higher positive tilts where it becomes more difficult to visibly distinguish each of the four discs. This is most likely due to the insufficient sampling with cone-beam acquisitions. Tuy's data sufficiency condition requires that each plane passing through the reconstructed region of the object must intersect the orbit of the focal point trajectory at least once. Due to the failure to meet this condition, reconstruction of slices for locations farther away from the flat plane of the beam contain significant distortion and errors. In this case, when the CmT detector is down (closer to the ground) at a -10° tilt (refer to Appendix B, Fig. 8, LEFT), the cone-beam is relatively flat near the top. At this top slice, there is nearly complete sampling and the discs near the top appear to be less distorted. The reverse is true in the +10° tilt case (refer to Appendix B, Fig. 9, LEFT), where the insufficient sampling occurs near the top since at this location the rays diverge away from the flat plane of the cone-beam which is now near the bottom of the reconstructed images. However, this limitation can be overcome by using a 3D complex acquisition trajectory such as saddle. As shown in the reconstructed slices, the tilted acquisition orbits show distortion in the discs in planes away from the flat plane of the cone-beam, while the saddle trajectory shows the least disc distortion due to the more complete volumetric cone-beam sampling.

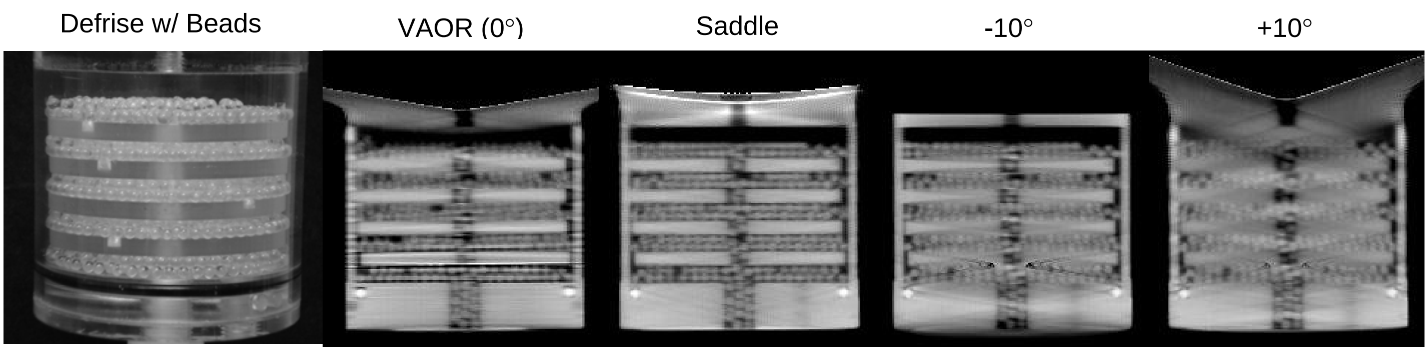

FIGURE 1. (LEFT) Photograph of the Defrise phantom with 3.5mm acrylic beads between the gaps between the discs. (RIGHT images) Reconstructed images acquired with vertical axis of rotation (VAOR), Saddle, and ±10° acquisition trajectories.

Despite the apparent distortion in the discs, the image reconstructions of the small acrylic beads can still easily be picked out and appear to be less distorted even in regions where the data might not be completely sampled. This can be clearly seen in the bottom area of the reconstructed images of the center region of the Defrise phantom. This finding suggests that despite incomplete sampling, small objects (i.e. acrylic beads) remain more preserved than larger low frequency information (i.e. geometrically uniform discs). Therefore, the frequency content of the object also plays a role in object image recovery in the acquisition and reconstruction process.

These results shown here and Appendix B indicate that by having the cone-beam flat near the patient bed allows for more complete sampling near the chest wall. The drawback is that there are overlapping structures, geometric distortion, and incomplete sampling in the rest of the reconstruction volume for the tilted orbit acquisition. Based on these results, a tilt of 6.2° for the CmT sub-system was chosen since at this tilt the cone-beam is relatively flat at the top and a customized comfortable patient bed could fit above [5].

<u>*Unlisted Task: Integration of the two sub-systems*</u>

Although it was never written in the statement of works, a mounting plate had to be designed to integrate the independently developed SPECT and CmT sub-systems were onto a single gantry (Fig. 2). A custom designed ¼" aluminum plate was designed and mounted to the rotation stage. The SPECT system was mounted on this plate such that its center of rotation (COR) matched the COR of the rotation system. The plate was then reinforced with 1.5x3in^2 metal bars so that there would be enough support to hold the weight of both imaging systems. Two 3x3in^2 metal bars were mounted on either end of the plate to secure the CmT tube and detector. The CmT system was laterally offset 5cm from the center of rotation to allow the imaging of a wide range of breast sizes. Somewhat differently from its independent prototype, the CmT sub-system was placed at a 60cm source-to-image distance (SID), 38cm source-to-object distance (SOD), and 6.2° stationary tilt in order to accommodate a comfortable patient bed. The magnification

FIGURE 2. Photograph of the prototype dual-modality dedicated breast imaging tomographic system with a customized patient bed. The SPECT system (center) is placed orthogonally to the CmT tube (right) and digital flat-panel detector (left). The superimposed arrows illustrate system motions (polar and ROR for SPECT, and azimuthal for SPECT and CmT). Note that the pendant breast is in the common FOV of each system.

of about 1.57 of an object at the center was kept the same as the independent prototype. The 3x3in^2 metal bars supporting the x-ray source and detector have the flexibility to adjust the SID, SOD, and detector and x-ray source tilt.

Task 1(a)

In this current configuration, the CmT system does not enter the field-of-view (FOV) of the SPECT projection view. However for the CmT projection images, the SPECT camera and motor is in the FOV at all positions. To ensure that the SPECT sub-system is not in close proximity to the object in the CmT FOV, the SPECT camera is set at a 40° polar tilt and zero ROR during CmT acquisition (Fig. 3, TOP LEFT). A study was done to see the effect on the reconstructed slices if the SPECT sub-system was obstructing the object in the CmT projections. At a higher tilt and larger ROR, the SPECT camera is more in the FOV and overlaps with the breast (Fig. 3, TOP RIGHT). In the reconstructed sagittal slices, an artifact due to the camera can be seen near the bottom of the breast (Fig. 3, BOTTOM RIGHT). The circular ring that is seen in the reconstructed images is due to the offset of the CmT system and methods to reduce this artifact will be further investigated in Task 2(a) in Year 2.

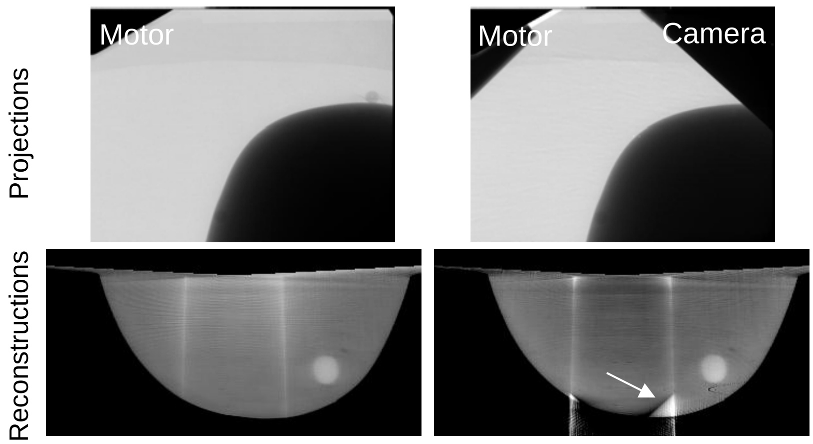

FIGURE 3. CmT (TOP) projections and (BOTTOM) reconstructions of a 900mL breast phantom with a CT-contrast filled lesion. Acquisitions were taken (LEFT) without and (RIGHT) with the SPECT camera obstructing the phantom. White arrow near the bottom of the breast shows the artifact due to the SPECT camera in the FOV.

Task 1(c)

An imaging sequence for the SPECT and CmT data acquisition was created such that a large breast volume (and possibly the chest wall) could be completely sampled and imaged without physical constraints in the FOV. Although simultaneous acquisition was preferred due to a shorter image acquisition time and easier image registration, the issue was that the SPECT camera and motor was in the FOV of the CmT projections (as described and shown in Task 1(a)) and a large portion of the breast could not be imaged by the CmT sub-system due to a higher bed height. Lowering the bed to allow more of the breast into the FOV would require having a limited image acquisition due to the physical dimensions of the x-ray tube and detector preventing a full 360°. Compared with a full 360° acquisition, SPECT reconstructed images collected with a limited acquisition did not show significant reduction in image quality. However, Figure 4 shows a definite loss of attenuation value in the CmT reconstructed images in portions where there was no data collection. In addition, the circular cylinder due to the offset and insufficient sampling also becomes more prominent in partial azimuthal acquisition. A detailed description of this work and results was presented at the *2007 IEEE Nuclear Science and Medical Imaging Conference* for which I was a co-author. A conference proceeding was submitted and is attached in Appendix C.

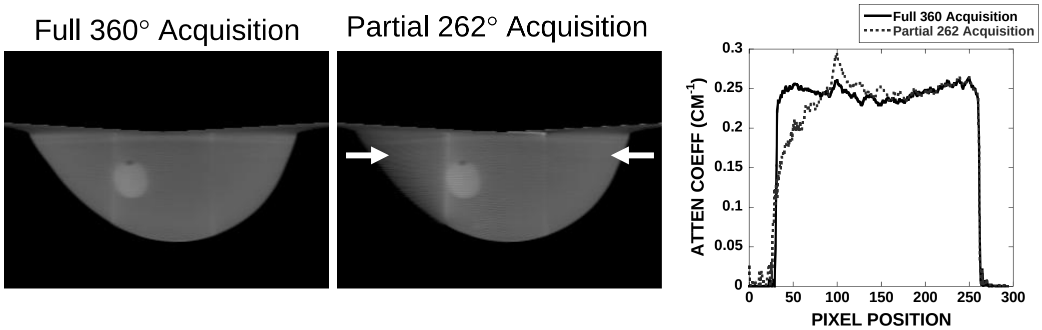

FIGURE 4. Reconstructed CmT image acquired with a (LEFT) 360° and (MIDDLE) 262° acquisitions. (RIGHT) Line profile was taken (white arrow) to show the loss of attenuation value in portions where the breast was undersampled in the 262° acquisition. Additionally, the circular offset is also more prominent in the CmT reconstructed image.

At the end, a sequential scan where SPECT and CmT images would be separately acquired was decided upon. Although this would take a longer time, CmT images could be taken at a different bed height without any emission contamination and physical constraints from the SPECT system. The inner trough of the patient bed was also removed to allow more of the breast to protrude into the FOV due to the larger hole in the table and weight of the patient. Below is the final sequence of events:

1. Due to the flexible positioning of the bed [6], the bed is first angled upward and then brought down as far as it can go without hitting the CmT tube.
2. After the breast is properly positioned into the FOV and the SPECT camera is set at a 40° polar tilt and zero ROR, a 360° CmT scan is acquired.
3. Patient is injected with radioactivity and a 360° SPECT acquisition is performed at a higher bed height such that the CmT system does not hit the bed. Various 3D complex acquisition trajectories can be used to contour and get closer to the breast and chest wall.

Task 1(b)

At present, the data acquisition sequences of both systems are independently automated on separate computers. The SPECT system uses custom-built software written in LabVIEW™ while the acquisition routine for the CmT system is implemented in C++. The future step will be to integrate both utilities into one program such that both systems can be controlled together from one computer during image acquisition. This software was originally promised to be written up by the end of Year 1. However, due to the complexities in the software and availability of computer processors, this task has taken longer than expected. I have currently been looking into integrating the CmT acquisition software into the custom-built LabVIEW™ program for SPECT. This will hopefully be implemented by the end of Year 2.

Unlisted Task: Imaging Feasibility of the hybrid system AND Task 3(a)

To evaluate the feasibility of this dedicated system, geometric phantoms were first acquired to study the sampling and resolution properties and demonstrate the fusion of the functional-anatomical images (Appendix D, Fig. 2). Although the CmT images showed slight distortion toward the edges and a circular ring artifact, images were registered using common features in both data sets. Image fusion was done using an open source *AMIDE* software [7, 8].

Images of a breast phantom with external fiducial markers were also acquired. Small and fixed external fiducial markers were used in order to ensure proper registration, be visible and distinguished in both systems, and not interfere with the images. After testing commercially available fiducial markers and plastic centrifuge vials filled with ^{99m}Tc and CT contrast agent, four 6.0mm nylon balls (*Small Parts, Inc.* Miami Lakes, FL) soaked in aqueous ^{99m}Tc-pertechnetate were used as markers and taped to the exterior surface of the breast phantom. With the help of these fiducial markers, the images from both systems were fused (Appendix D, Fig. 3). There was enough natural contrast between air and nylon to discriminate the fiducial markers in the CmT projections and reconstructed images. In volumetric 3D space, the SPECT reconstructed images were rotated 90° azimuthally (due to the position of the SPECT sub-system with respect to the CmT sub-system) and shifted downward (due to the different bed positions used for SPECT and CmT acquisitions). Fiducial markers made it possible to accurately perform these tasks so that the two data sets were aligned as close as possible.

In addition, a preliminary investigation on the clinical performance of the system was done by imaging two women with confirmed breast cancer: one on the independent SPECT system and the other on the SPECT-CT system. Although the SPECT images could see up to and past the chest wall (Appendix D, Fig. 4-6), there was limited visualization of the chest wall in the CT images (Appendix D, Fig 5-6), which remains an important consideration in planned refinements of the current hybrid system.

A detailed description of this entire work and results was presented at the *2007 IEEE Nuclear Science and Medical Imaging Conference* for which I was the primary author. A conference proceeding was submitted and is attached in Appendix D.

Task 4: Complete other aspects of the breast cancer training program

<u>Task 4(a)</u>

As of now, I have only observed a new breast cancer screening approach using random periareolar fine needle aspiration (rpFNA) which is done mostly in high-risk women. rpFNA is similar to pap-smear in that a sample of cells is collected from the entire breast. Patients were asked to lie on their backs on the table. For each breast, about 9 aspirations are taken from the outer (~9 o'clock) and inner side (~3 o'clock) near the nipple surface and areola. Before starting each side, the patient's breast is numbed with a couple of injections of an anesthetic. A needle is positioned in the same spot (fulcrum) as the anesthetic injection and moved around the fulcrum to collect random samples around the circumference of the squeezed breast. Once the sample is collected, the contents of the syringe are transferred to another tube with RPMI solution, which is used to prevent cells from sticking to each other. This is repeated 3 more times (using separate needles) with an additional needle injected in the outer side for fatty cell content. Another four samples are collected from the inner side and transferred to another set of tubes. This is repeated for the contralateral breast. The cell count in these tubes can vary from 5 to more than 5,000. Cold packs were applied to the breast and chest wall and women were asked to wear a sports bra to minimize any breast movement. For each breast, the procedure took about 15 minutes. Cells from the outer, inner, left and right breast are processed separately. For each side, samples are collected in two tubes to test correlation and examine for abnormality.

I plan on continuing to observe additional clinical aspects in breast cancer imaging for the remaining two years.

<u>Task 4(d)</u>

Research work that has been shown here has been presented at *SPIE Medical Imaging Conference* and *IEEE Nuclear Science and Medical Imaging Conference*. I also attended the *Society of Nuclear Medicine Conference* and *Radiological Society of North America Conference* which was a great experience. Although I did not present any of my research work, it was a great to see the clinical aspects of medical imaging. I plan on attending these same and other conferences in the next two years.

C. KEY RESEARCH ACCOMPLISHMENTS

Year 1 included Tasks 1(a)-(c) and 4(a) from the original statement of works (Appendix A). However, Task 1(b) was not completed due to the complexity of combining the softwares of the two systems. This will now be done in Year 2. Instead, Task 1(d) and Task 3(a), which were promised in Year 2, were completed. Below is a specific summary of the progress that has been made.

- Since the limiting factor in designing a customized patient bed was the CmT system, the evaluation of lesion distortion, reconstruction artifacts, and sampling insufficiency in CmT images at different tilts were first explored. A 6.2° tilt was decided upon since the cone-beam is nearly flat at the top near the patient bed which allows more complete sampling of the breast near the chest wall (Appendix B).
- Using a 3D CAD program, *Autodesk Inventor*, the hybrid system was designed and built.
- A customized patient bed specific for this hybrid system was built. I was a co-author for this work.
- An optimal imaging sequence protocol was developed (Appendix C).
- Using the hybrid system, customized patient bed, and imaging sequence, the first hybrid patient study was conducted. CmT images showed limited visualization of the patient wall but with improved patient

imaging this will hopefully not be a problem. These results have and will be presented at various conferences (Appendix D). In the next few months, more patient studies using the hybrid system will be performed.

- Task 4(a) is still currently in progress. I have only observed a new breast cancer screening approach using rpFNA. I plan on continuing to observe additional clinical aspects in breast cancer imaging for the remaining two years.
- Work has been presented at various conferences and future work will also be presented in upcoming conferences.

<u>*Related*</u>

- Results from this work were presented in my preliminary proposal, “Development and Optimization of a Dedicated Dual-Modality SPECT-CmT System for Improved Breast Lesion Diagnosis”, which was accepted by my dissertation committee on July 19, 2007.

D. REPORTABLE OUTCOMES

Conference Proceedings

DJ Crotty, **P Madhav**, RL McKinley, MP Tornai. “Investigating novel patient bed designs for use in a hybrid dual modality dedicated 3D breast imaging system.” Presented at the *2007 SPIE Medical Imaging Conference*, San Diego, CA, 17-22 Feb. 2007 and to be published in *Proc. SPIE: Physics of Medical Imaging*, 6510:H1-10.

P Madhav, DJ Crotty, RL McKinley, MP Tornai. “Evaluation of lesion distortion at various CT system tilts in the development of a hybrid system for dedicated mammotomography.” Presented at the *2007 SPIE Medical Imaging Conference*, San Diego, CA, 17-22 Feb. 2007 and published in *Proc. SPIE: Physics of Medical Imaging*, 6510:F1-12.

KL Perez, **P Madhav**, DJ Crotty, MP Tornai. “Analysis of patient bed positioning in SPECT-CT imaging for dedicated mammotomography.” Presented at the *2007 SPIE Medical Imaging Conference*, San Diego, CA, 17-22 Feb. 2007 and to be published in *Proc. SPIE: Physics of Medical Imaging*, 6510:371-8.

P Madhav, SJ Cutler, KL Perez, DJ Crotty, RL McKinley, TZ Wong, MP Tornai. “Initial patient study with dedicated dual-modality SPECT-CT mammotomography.” Presented at the *2007 IEEE Nucl. Sci. Symposium & Med. Imaging Conference*, Honolulu, Hawaii, 28 Oct.-3 Nov. 2007 and published in *IEEE Conference Record NSS/MIC*, 5:3781-3787.

SJ Cutler, **P Madhav**, KL Perez, DJ Crotty, MP Tornai. “Comparison of reduced angle and fully 3D acquisition sequencing and trajectories for dual-modality mammotomography.” Presented at the *2007 IEEE Nucl. Sci. Symposium & Med. Imaging Conference*, Honolulu, Hawaii, 28 Oct.-3 Nov. 2007 and published in *IEEE Conference Record NSS/MIC*, 6:4044-4050.

Abstracts and Presentations

DJ Crotty, **P Madhav**, KL Perez, SJ Cutler, RL McKinley, T Wong, PK Marcom, MP Tornai. “3D molecular breast imaging with dedicated emission mammotomography: results of the first patient study.” Presented at the *Duke University Center for Molecular and Biomolecular Imaging Meeting*, Durham, NC, 11-13 March, 2007 and *Duke Frontiers 2007*, Durham, NC, 14 May, 2007.

P Madhav, DJ Crotty, SJ Cutler, KL Perez, RL McKinley, MP Tornai. “A novel dual-modality SPECT-CT system dedicated to 3D volumetric breast imaging.” Presented at the *Duke University Center for Molecular and Biomolecular Imaging Meeting*, Durham, NC, 11-13 March, 2007 and *Duke Frontiers 2007*, Durham, NC, 14 May, 2007.

MP Tornai, **P Madhav**, DJ Crotty, SJ Cutler, RL McKinley, KL Perez, JE Bowsher. “Initial hybrid SPECT-CT system for dedicated fully-3D breast imaging.” Presented at the *2007 Society of Nuclear Medicine Meeting*, Washington, DC, 2-6 Jun. 2007, and published in J. Nucl. Med. 48(5). 2007.

MP Tornai, **P Madhav**, DJ Crotty, SJ Cutler, RL McKinley, KL Perez, JE Bowsher. “Application of volumetric molecular breast imaging with a dedicated SPECT-CT mammotomograph.” Presented at the *2007 American Association of Physicists in Medicine Meeting*, Minneapolis, MN, 22-26 Jul. 2007, and published in Med. Phys. 34(6):2597.

P Madhav, SJ Cutler, DJ Crotty, KL Perez, RL McKinley, MP Tornai. “3D volumetric breast imaging with a dedicated dual-modality SPECT-CT system.” Presented at the *2007 Duke Biomedical Engineering Retreat*, Myrtle Beach, SC, 7-9 Oct. 2007.

P Madhav, MP Tornai. “Development and optimization of a dedicated, hybrid dual-modality SPECT-CmT system for improved breast lesion diagnosis.” To be presented at the *2008 Era of Hope Conference*, Baltimore, MD, 25-28 Jun 2008.

Funding

Received a registration fee waiver from SPIE - The International Society for Optical Engineering and the Symposium and Conference Chairs of the Medical Imaging to attend the *2007 SPIE Medical Imaging Conference* in San Diego, CA and present results for my submitted and accepted abstract.

Received a $500 Conference Travel Fellowship from Duke University’s Graduate School to help pay for costs to attend the *2007 IEEE NSS/MIC Conference* in Honolulu, Hawaii and present results for my submitted and accepted abstract.

Received a registration fee waiver from the 2007 IEEE MIC Travel Grant to attend the *2007 IEEE NSS/MIC Conference* in Honolulu, Hawaii and present results for my submitted and accepted abstract.

E. CONCLUSION

A hybrid dual-modality SPECT-CmT system for dedicated breast imaging was built. The effect of reconstructed images at various CmT system tilts was investigated to find an optimal tilt that would completely sample a pendant, uncompressed breast and fit over a customized patient bed. In the end, it was decided that a 6.2° tilt would be optimal since it would completely sample the breast near the chest wall. Investigation of the SPECT physical constraints on the CmT images led to the development of a sequential data acquisition protocol for the SPECT-CmT system. Using this protocol, sampling/resolution properties and image registration with the use of external fiducial markers were performed. This was further extended to using the hybrid system to acquire data from a patient with confirmed breast cancer. In addition, other breast cancer detection protocols outside my research area were observed to learn different aspects in this field.

F. REFERENCES

[1] D. J. Crotty, C. N. Brzymialkiewicz, R. L. McKinley, and M. P. Tornai, "Optimizing orientation of SPECT and CT detectors through quantification of cross contamination in a dual modality mammotomography system," *2005 IEEE Nucl Sci Symp & Med Imag Conf,* vol. 3, pp. 1672-1676, 23-29 Oct. 2005.

[2] D. J. Crotty, C. N. Brzymialkiewicz, R. L. McKinley, and M. P. Tornai, "Investigation of emission contamination in the transmission image of a dual modality computed mammotomography system," *2006 Proc SPIE: Phys Med Imag,* vol. 6142, pp. 664-674, 11-17 Feb. 2006.

[3] R. L. McKinley, C. N. Brzymialkiewicz, P. Madhav, and M. P. Tornai, "Investigation of cone-beam acquisitions implemented using a novel dedicated mammotomography system with unique arbitrary orbit capability," *2005 Proc SPIE: Phys Med Imag,* vol. 5745, pp. 609-617, 12-18 Feb. 2005.

[4] P. Madhav, D. J. Crotty, R. L. McKinley, and M. P. Tornai, "Evaluation of lesion distortion at various CT system tilts in the development of a hybrid system for dedicated mammotomography," *2007 SPIE Med Imag Conf,* vol. 6150, 2007.
[5] D. J. Crotty, P. Madhav, R. L. McKinley, and M. P. Tornai, "Patient bed design for an integrated SPECT-CT dedicated mammotomography system," in *2006 Workshop on the Nuclear Radiology of Breast Cancer*, San Diego, CA, 2006.
[6] K. L. Perez, P. Madhav, D. J. Crotty, and M. P. Tornai, "Analysis of patient bed positioning in SPECT-CT imaging for dedicated mammotomography," *2007 SPIE Med Imag Conf,* vol. 6510, pp. 371-8, 2007.
[7] A. M. Loening and S. S. Gambhir, "AMIDE: a free software tool for multimodality medical image analysis," *Mol. Imaging,* vol. 2, pp. 131-137, 2003.
[8] D. Stout, "Multimodality image display and analysis using AMIDE," *J Nucl Med,* vol. 48, p. (Supplement 2) 205P, 2007.

APPENDIX A: STATEMENT OF WORK

Task 1 Design and implement a dual-modality prototype system (Months 1-17):

a. Investigate effect of physical constraints (such as having the SPECT camera partially in front of the x-ray detector) on scatter contamination in reconstructed images. (Months 1-5)
b. Develop software to synchronize both systems during image acquisition. (Months 6-11)
c. Develop an ideal sequence (based on complete sampling, physical constraints) for emission and transmission data acquisition. (Months 11-12)
d. Explore 3D complex orbits with physically possible optimal orientations and tilt angles that can be used to have the system fit underneath the patient bed and still be able to image close to the chest wall. (Months 13-17)

Task 2 Optimize CmT system by applying corrections to improve image quality (Months 18-29):

a. Investigate methods to reduce circular artifacts in reconstruction from CmT images collected with a centered object and laterally offset central x-ray beam. (Months 18-22)
b. Investigate and implement scatter correction methods to CmT images. (Months 23-29)

Task 3 Evaluate SPECT system for quantification measurements of lesion activity (Months 22-36):

a. Perform image registration of SPECT and CmT images using existing image registration algorithm (i.e. surface fitting technique) with the aid of fiducial markers. (Months 22-23)
b. Investigate, implement, and compare two attenuation correction methods (i.e. uniform attenuation distribution, CmT-based attenuation distribution) to apply to SPECT data. (Months 24-30)
c. Perform SPECT quantification measurements incorporating all corrections using phantoms and lesions with known concentration activity. (Months 30-36)

Task 4 Complete other aspects of the breast cancer training program (Months 1-36):

a. Shadow a radiologist(s) to observe the clinical and diagnostic side in breast cancer imaging (Nuclear Medicine, Mammography). (Months 1-12)
b. Publish research work in peer-reviewed journals. (Months 1-36)
c. Attend and present at local seminars offered at Duke University through Medical Physics and the Breast and Ovarian Oncology Research Program, which is part of the Duke Comprehensive Cancer Center. (Months 13-36)
d. Attend international conferences such as SPIE Medical Imaging Conference, DOD BCRP Era of Hope Meeting, IEEE Medical Imaging Conference, RSNA Conference, and San Antonio Breast Cancer Symposium. (Months 13-36)
e. Prepare thesis and defend. (Months 30-36)

APPENDIX B: 2007 SPIE MEDICAL IMAGING CONFERENCE RECORD

Evaluation of Lesion Distortion at Various CT System Tilts in the Development of a Hybrid System for Dedicated Mammotomography

Priti Madhav[1,2], Dominic J. Crotty[1,2], Randolph L. McKinley[1,2], Martin P. Tornai[1,2]

[1] Department of Radiology, Duke University Medical Center, Durham, NC
[2] Department of Biomedical Engineering, Duke University, Durham, NC

ABSTRACT

A hybrid SPECT-CT system for dedicated 3D breast imaging (mammotomography) is currently under development. Each imaging system will be placed on top of a single rotation stage and moved in unison azimuthally, with the SPECT system additionally capable of polar and radial motions. In this initial prototype, the CT system will initially be positioned at a fixed polar tilt. Using a phantom with three tungsten wires, the MTF of the CT system was measured in 3D for different CT system tilts. A phantom with uniformly arranged 0.5cm diameter acrylic spheres was suspended in air in the CT field of view, and also placed at multiple locations and orientations inside an oil-filled breast phantom to evaluate the effect of CT system tilt on lesion visibility and distortion. Projection images were collected using various simple circular orbits with fixed polar tilts ranging between ±15°, and complex 3D saddle trajectories including combined polar and azimuthal motions at maximum polar tilt angles. Reconstructions were performed using an iterative reconstruction algorithm on 4x4 binned projection images with 0.508mm^3 voxels. There was minor variation in the MTF in the imaged volume for the CT system at all trajectories, potentially due to the use of an iterative reconstruction algorithm. Results from the spherical cross phantoms indicated that there was more reconstruction inaccuracy and geometric distortion in the reconstructed slices with simple circular orbits with fixed tilt in contrast to complex 3D trajectories. Line profiles further showed a cupping artifact in planes farther away from the flat plane of the x-ray cone beam placed at different tilts. However, this cupping artifact was not seen for images acquired with complex 3D trajectories. This indicated that cupping artifacts can also be caused by undersampled cone beam data. These findings generally indicate that despite insufficient sampling with the cone beam imaging geometry, it is possible to place the CT system at a stationary polar tilt with the CT tube positioned upward such that a patient can be comfortably placed above the system and allow complete sampling near the top of the pendant, uncompressed breast and chest wall. However, a complex 3D trajectory allows for more complete sampling of the entire image volume.

Keywords: computed tomography, tomography, mammotomography, breast imaging, transmission imaging, cone beam, dual –modality, orbits, iterative reconstruction, modulation transfer function (MTF)

1. INTRODUCTION

Over the past decade, dual-modality tomographic imaging systems have grown in popularity and offer great promise in the detection and staging of numerous cancerous diseases, monitoring and prediction of treatment therapies, and improving precision of surgical biopsies. The main benefit of simultaneously acquiring 3D transmission and emission data is in the ability to fuse the structural anatomical framework of an object obtained from a transmission image onto an emission image that illustrates the localization of the radioactive metabolic uptake (i.e. function) of a tumor. Additionally, the transmission data can be used to estimate an attenuation map of the object and can be applied to the emission data to compensate for photon attenuation and absorption by overlapping structures. It is expected that integrating complementary anatomical and functional information can lead to further improvement in visual quality and quantitative accuracy of radionuclide imaging over independent systems[1-5].

Our lab has been working on developing such a dual-modality single photon emission computed tomography (SPECT) and computed mammotomography (CmT) imaging system specifically dedicated to fully-3D breast imaging[6-8]. With the compact, high performance gamma camera of the SPECT system[9] and novel quasi-monochromatic x-ray cone beam of the CmT system[10, 11], both systems have independently yielded visualization of small lesions in the breast, especially ones closer to the chest wall. The 3D motion positioning of each system allows the detector to be positioned anywhere about a pendant, uncompressed breast[10, 12-14]. 3D acquisition trajectories have been implemented to contour the breast and image further into the breast by utilizing the system's azimuthal and polar tilting capabilities.

In its initial integration, the SPECT system retains its fully 3D positioning. However, the CmT system is at a fixed tilt angle and restricted to the 360° azimuthal direction around the vertical axis of a pendant breast. This limits the CmT system in imaging deep into the breast and axillary region, and introduces insufficient sampling which was previously shown by us to be overcome by using 3D complex acquisition trajectories[12]. In this study, we describe the configuration of the dual-modality SPECT-CmT system and quantify the effects of spatial resolution and lesion distortion of the CmT system at different stationary tilts and 3D complex acquisition trajectories. It is necessary to find a stationary tilt that will provide sufficient information and allow maximal access to the patient's breast, and accommodate a custom patient bed that can fit above this compact hybrid system and shield the patient from scattered, low energy x-rays and photons, and maintain patient comfort[15].

2. MATERIALS AND METHODS

2.1. Overview of the SPECT-CmT System

The first prototype compact dual-modality SPECT-CmT system was built (Fig. 1) to image a pendant uncompressed breast[6]. Both systems, using separate detectors to view an object in the common field-of-view (FOV), rest on top of a common rotation stage (model RV350CCHL, *Newport Corp.*, Irvine, CA) to allow an azimuthal rotation of 360° around the vertical axis of the breast. The SPECT system is placed at a fixed position such that it is 90° relative to the x-ray source-detector axis, and the center of rotation (COR) matches the COR of the CmT system. With both systems on the same gantry, the patient will not be required to move between the SPECT and CmT acquisitions. A customized patient bed, which will be placed above the hybrid system, is currently being designed such that it will maintain patient comfort and allow the imaging systems to contour the patient's breast[15].

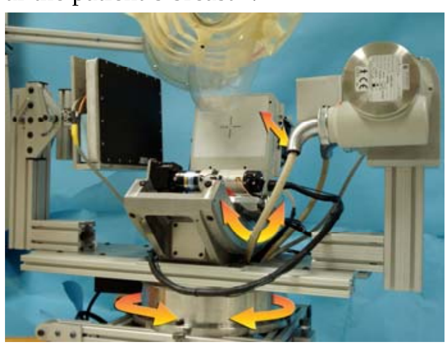

Figure 1: Photograph of the prototype dual-modality dedicated breast imaging tomographic system. The SPECT system (center) is placed orthogonally to the CmT tube (right) and digital flat-panel detector (left). The arrows illustrate system motions (azimuthal, polar, and radius of rotation). Note that the pendant breast is in a common FOV of each system.

Figure 2 shows a few images of the current dual-modality SPECT-CmT system rotating around a pendant uncompressed breast. As shown in the corresponding polar plot, the SPECT system has its fully 3D positioning capabilities while the CmT system remains at a fixed polar tilt as the system rotates 360° around the breast.

Along with the parallel beam imaging geometry of the SPECT system, the entire volume of the breast is in the FOV of both systems even at different cone beam CmT tilts. This is shown in the 3D CAD drawings of the SPECT-CmT system in Fig. 3. Additionally, in order to completely sample the entire volume of interest, the central ray of the CmT cone beam is laterally offset 5cm relative to the center of rotation[11].

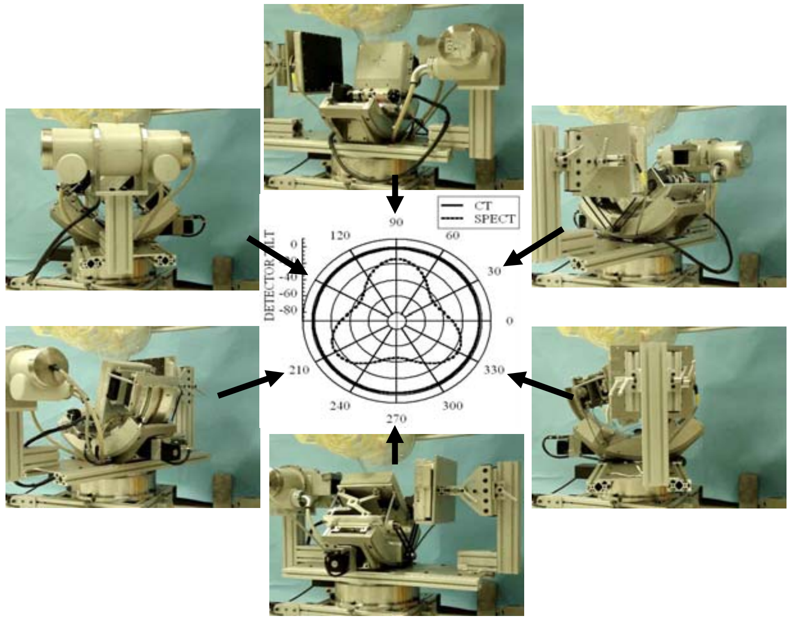

Figure 2: Photographs at different positions of the dual-modality system rotating around a pendant, uncompressed phantom breast and torso. Polar plot (center) is shown for the SPECT (3D PROJSINE orbit is dotted) and CmT systems (vertical axis of rotation [VAOR] orbit is solid circle).

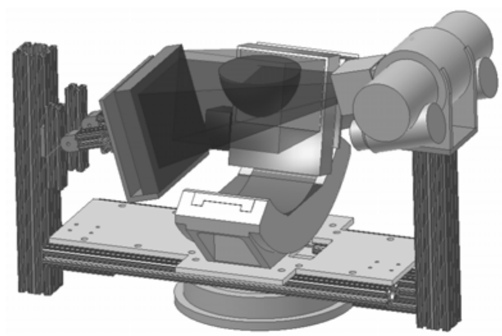

Figure 3: 3D CAD model of the SPECT-CmT system with a breast placed at the center of rotation of the system. The breast is in the FOV of both systems regardless of the tilt of the CmT system (-15 degrees shown in this diagram). This is shown with the intersection of both the parallel beam of the SPECT system and the cone beam of the CmT system.

2.2. SPECT System

Our current emission tomography system uses a compact 16x20cm^2 field of view Cadmium Zinc Telluride (CZT) gamma camera (model *LumaGEM* 3200S^{TM}, *Gamma Medica, Inc.*, Northridge, CA) with discretized crystals, each 2.3x2.3x5mm^3 on a 2.5mm pitch. Measured energy resolution of the gamma camera at 140keV is 6.7% FWHM and collimator sensitivity is 37.9cps/MBq[13]. Higher energy resolution is the primary reason of using the CZT camera over scintillators such as the NaI(TI)-based cameras for the SPECT system. This system has a parallel-hole collimator with hexagonal holes (1.2mm hole size flat-to-flat, 0.2mm septa, and 25.4mm height). The camera is attached to a laboratory jack and a goniometric cradle (model BGM200PE, *Newport Corp.*, Irvine, CA) permitting various radius of rotations (RORs) and polar tilts (φ), respectively.

2.3. CmT System

Our existing cone beam transmission tomography system uses a rotating tungsten target x-ray source (model *Rad-94*, *Varian Medical Systems*, Salt Lake City, UT) with a 0.4/0.8mm focal size and 14° anode angle and a 20x25cm^2 FOV CsI(T1)-based amorphous silicon digital x-ray detector (model *Paxscan 2520*, *Varian Medical Systems*, Salt Lake City, UT) with a grid size of 1920x1536pixels and 127µm pitch. Source and detector are secured to the same metal plate as the SPECT system. A custom built collimator is attached to the x-ray source to hold ultra-thick K-edge beam shaping filters to produce a quasi-monochromatic beam[16]. For these studies, a Ce 100th attenuating value layer filter (Z=58, ρ=6.77g/cm^3, K-edge=40.4keV, *Santoku America, Inc.*, Tolleson, AZ) was used to yield a mean energy of ~36keV and FWHM of 15%. In the hybrid setup, the source-to-image distance (SID) was 60cm and source-to-object distance (SOD) was 38cm. The central ray of the CmT cone beam is laterally offset 5cm relative to the center of rotation to completely sample the entire volume of interest[11]. Unlike the SPECT system, the CmT system is at a fixed tilt angle and restricted to only azimuthal motion.

2.4. Phantoms

The MTF in 3D was calculated using an MTF thin-wire phantom as previously described[17] (Fig. 4, LEFT). Three tungsten wires of 508µm diameter and ~11cm length were positioned nearly orthogonal to each other within the cube such that they were visibly separable in their positions and did not touch each other near the center.

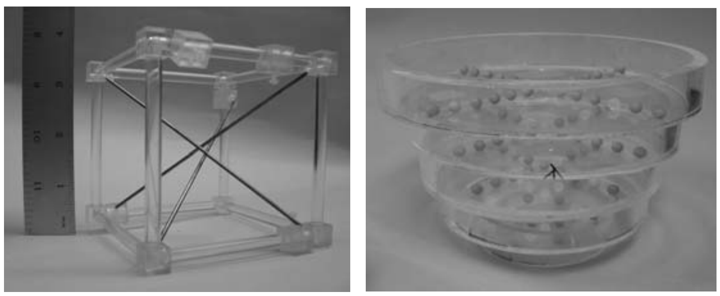

Figure 4: (LEFT) Photograph of the MTF phantom used to measure the MTF in 3D. (RIGHT) Photograph of the phantom with small spheres suspended on thin plastic sheets inside each circular band; each sphere is a 0.5cm diameter acrylic ball arranged in a cross pattern to measure lesion visualization at different planes in an image volume.

To measure the lesion visualization and distortion at different planes of the image volume, a phantom consisting of multiple circular acrylic bands of varying diameters and 2cm height were constructed (Fig. 4, RIGHT). Plastic wrap ("Saran") with 0.5cm diameter acrylic balls arranged on a 1cm center-to-center pitch in a cross pattern using a jig was stretched and glued to the bottom of each circular frame. The completed frames could then be easily stacked and also immersed in liquids while retaining the distribution of spheres on a single plane.

2.5. Data Acquisition

For the MTF and lesion distortion evaluation experiments, the independent CmT system was used in its original goniometric configuration[10-12]. In this setup, the source-to-image distance (SID) was 55cm and the source-to-object distance (SOD) was 35cm. Tube potential was set at 60kVp with a 1.25mAs exposure. MTF was measured by suspending the MTF phantom in air at the COR of the CmT system. Tilt effects were also evaluated by stacking the multiple spherical cross phantoms in a 1050mL breast phantom shell (nipple-to-chest distance of 11cm, medial-to-lateral distance of 17cm, and superior-inferior distance of 18cm). These measurements were taken in air and with the breast uniformly filled with mineral oil to provide different contrasts between the acrylic spheres and breast background. Mineral oil has an intrinsic density of 0.87 g/cm^3 and acrylic has a density of 1.19 g/cm^3.

Initial measurements were obtained using a simple circular trajectory at 0, ±5, ±10 and ±15 degree fixed polar tilts (Fig. 5, LEFT), and a saddle trajectory having +15 to -15 degree polar tilt (Fig. 5, RIGHT). Note that a negative polar tilt is defined as the x-ray source moving up (closer to the patient bed) and the detector moving down (closer to the ground). Projection images were collected every 1.5° through a 360° azimuthal acquisition for a total of 240 projections. Although the breast is truncated (as shown in the 3D CAD drawings), the spherical cross phantoms were placed in the breast such that they were in the center of the field-of-view and not truncated.

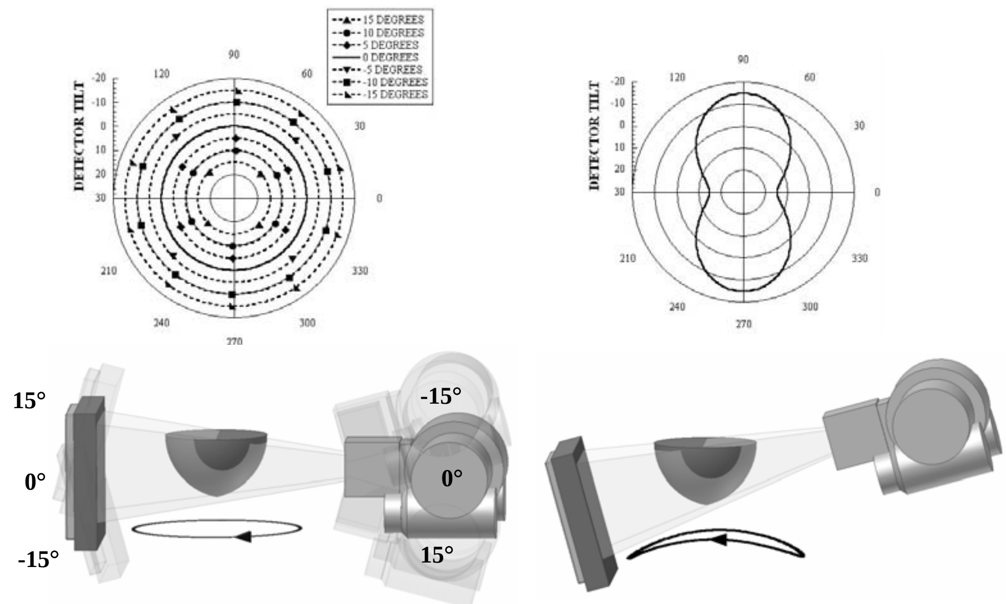

Figure 5: (TOP) Polar plots for (LEFT) simple circular trajectories at 0, ±5, ±10, and ±15 degree fixed polar tilts and (RIGHT) 3D saddle trajectories. Polar tilt of the CmT system is defined by the radius of the circle, and azimuth angle is defined around the circumference of the circle. (BOTTOM) The 3D CAD drawings of the setup of the CmT system are shown to illustrate the location(s) of the system during the acquisition. Negative polar tilt is defined as the x-ray detector moving down (or x-ray source moving closer to the patient bed). The breast phantom is placed in the cone beam CmT's FOV, and is seen to be laterally truncated somewhat in the drawings. Dark circles underneath CAD drawings indicate polar displacement with changing azimuth.

2.6. Image Reconstruction

Image reconstruction was performed on the CmT projection images using a statistically based iterative, ray-driven ordered-subsets transmission algorithm (OSTR)[10, 11, 16]. Projection images were corrected for gain and offset and binned to 4x4 pixels. Reconstruction parameters for the MTF acquisition were set to 10 iterations, 8 subsets, 350x350x384 reconstruction grid, and 508μm^3 voxel size. Reconstruction parameters for the lesion distortion measurements were set to 5 iterations, 16 subsets, 350x350x384 reconstruction grid, and 508μm^3 voxel size.

2.7. Data Analysis

Using an algorithm described previously[17], reconstructed images of the MTF phantom were used to calculate the MTF at different locations along each of the three wires. The MTFs were compared among the different acquisition orbits.

Lesion visualization and distortion were observed using the reconstructed images of the circular discs phantom collected for all acquisition orbits. For each circular disc, line profiles were drawn over the lesions in the horizontal and vertical directions. For each circular disc placed in oil, the line profiles obtained through the spheres were fit to a Gaussian curve and fit parameters extracted. Although the full-width at half maximum (FWHM) only partially characterizes the spatial resolution, it can be useful in making comparisons among different acquisition techniques such as CmT system tilts. Another useful parameter was the sphere's centroid which could be compared to the known 1cm pitch on the original phantoms.

3. RESULTS AND DISCUSSION

3.1. MTF in 3D

As shown in Figure 6 and Table I, there was no significant difference between the MTFs. As shown previously[17], the MTF does show improvement when the sampling rate is increased by binning the original projection images to 2x2 rather than 4x4. However, with the limitations in computer processor speed and memory, the current iterative reconstruction code can only handle 4x4 binned uncropped image sets and reconstruct to a limited grid size.

Since MTF measurements were taken using wires made of a highly attenuating material placed in air, there is a large difference in attenuation coefficients between the wire and background in the projection images. At each iteration, the nonlinear reconstruction algorithm maximizes this difference between pixel values and therefore a similar answer is obtained for all acquisition trajectories in just a few iterations. Thus, a similar study needs to be done to investigate the MTF when the phantom is instead placed in a scatter media (e.g. oil, water) such that there is not a large difference in attenuation values with tungsten and to add background noise.

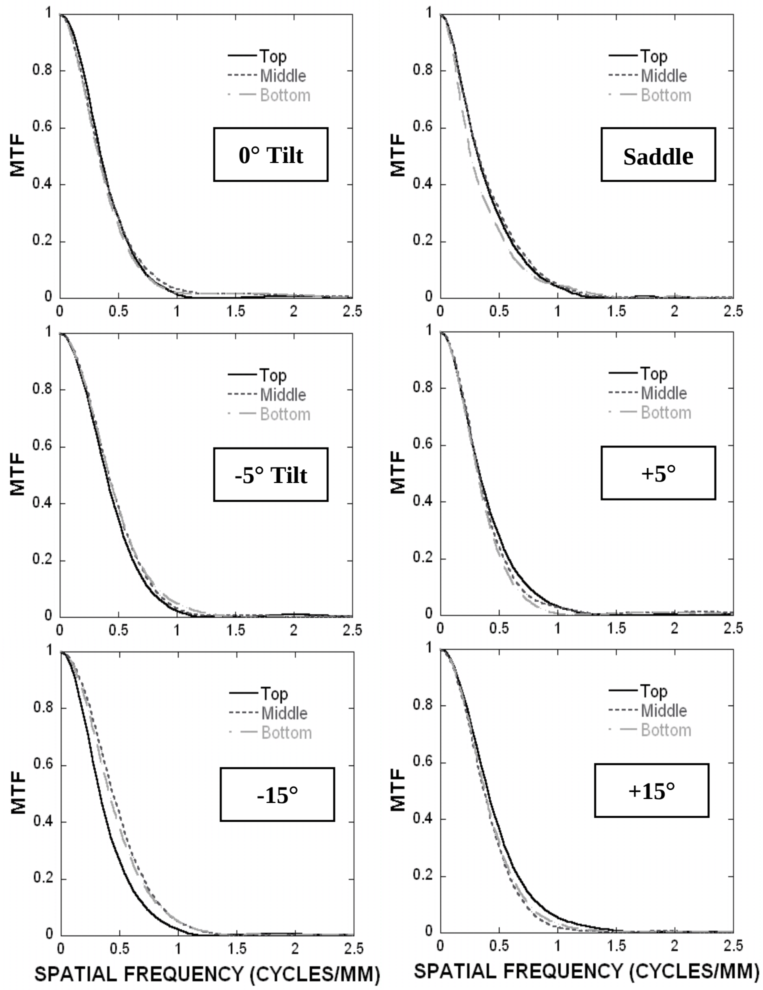

Figure 6: Measured MTF of the top, middle, and bottom part for Wire C for (TOP LEFT) 0, (MIDDLE) ±5, and (BOTTOM) ±15 degrees and (TOP RIGHT) saddle trajectory

Table 1: RMSD values along the top, middle, and bottom segment of each of the three tungsten wires for various acquisition trajectories

	Wire A		**Wire B**		**Wire C**	
Orbits	**Top-Middle**	**Middle-Bottom**	**Top-Middle**	**Middle-Bottom**	**Top-Middle**	**Middle-Bottom**
-15	0.020	0.011	0.019	0.018	0.045	0.015
-5	0.007	0.023	0.021	0.016	0.015	0.006
0	0.011	0.012	0.014	0.026	0.015	0.012
5	0.014	0.025	0.018	0.013	0.014	0.014
15	0.014	0.011	0.017	0.023	0.010	0.008
Saddle	0.021	0.010	0.022	0.011	0.009	0.026

3.2. Lesion Visualization/Distortion

Lesion distortion was first measured in different coronal slices of the breast phantom by obtaining line profiles over the acrylic balls in each circular phantom disc. Profiles were drawn through the lesions in each of the three smallest circular discs placed closest to the nipple (Fig. 7). From these profiles, it is seen that there is not much difference between the profiles for the spherical cross phantoms regardless of which acquisition trajectory (fixed tilt or saddle) was used.

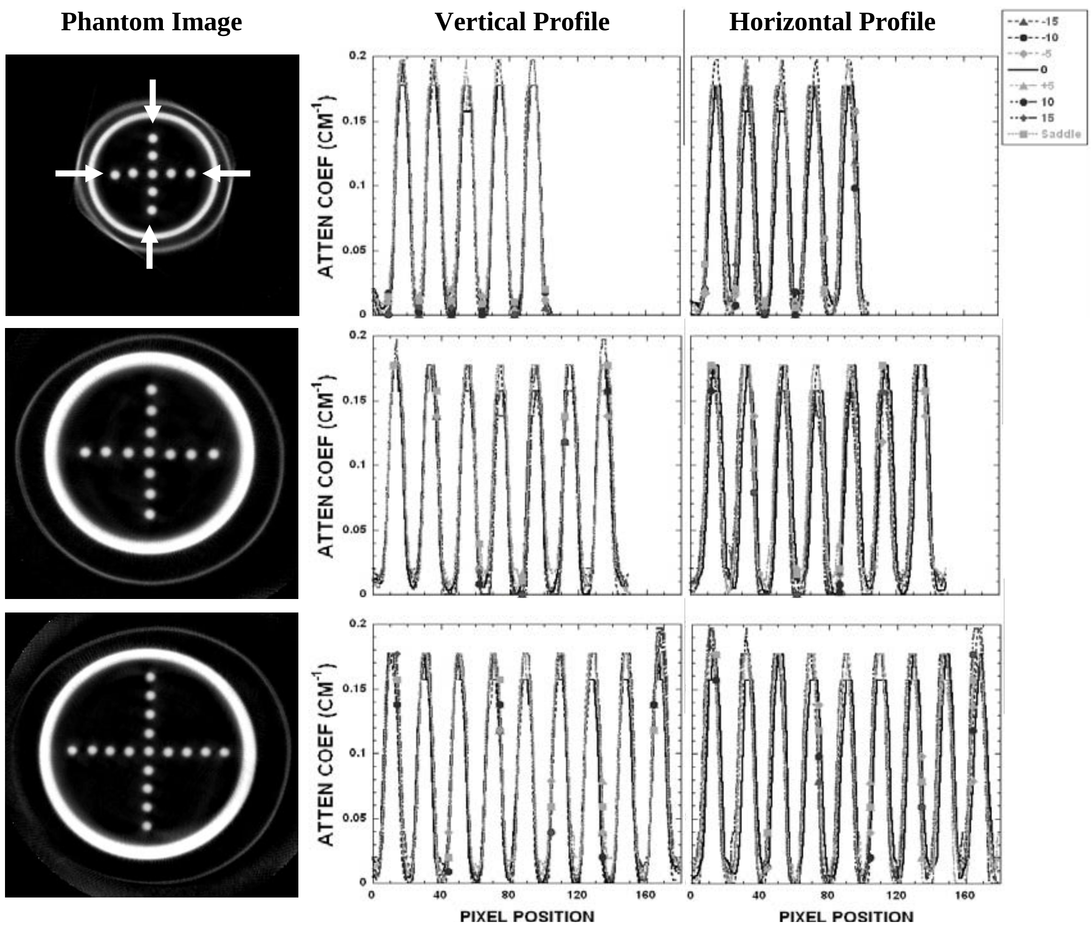

Figure 7: (LEFT) Reconstructed slices of the sphere phantoms acquired with saddle. (MIDDLE) Vertical and (RIGHT) horizontal profiles drawn through lesions at the level indicated by the white arrows in the top image plane.

By examining the reconstructed coronal slices at each of the circular discs, overlapping structures are apparent for reconstructed slices obtained using stationary polar tilt orbits (Fig. 8 and Fig. 9). Due to the failure to meet Tuy's data sufficiency condition in the polar direction for fixed tilt orbits[18], reconstruction of slices for locations far away from the flat plane of the cone beam contains errors due to insufficient sampling. This can be best explained in the 3D drawings. As shown in Fig. 8, when the CT detector is down (closer to the ground) at a -10° tilt, the cone beam is relatively flat at the top. At this slice, there is nearly complete sampling where we can see all the lesions and no overlapping structures (Fig. 10). However, as we look at reconstructed slices closer to the nipple, overlapping structures become more noticeable. At this tilt, each ray of the cone beam intersects the phantom in a similar way regardless of the azimuthal source-detector location. Due to the insufficient polar sampling to "fill in" additional views of the object in the FOV, out of plane information is inaccurately superimposed on any single plane of interest. The same is true in the +10° tilt case, whereas the reconstruction inaccuracy occurs for slices that are reconstructed from divergent cone beams rays away from the flat plane at the bottom of the cone beam (Fig. 9). Reconstruction inaccuracy would generally increase with larger cone beam angles. In addition to reconstruction inaccuracy, geometric distortion also results with circular orbits[12]. However, using the saddle trajectory, there is more complete polar sampling yielding far fewer noticeable artifacts in the reconstructed slices (Fig. 8 and Fig. 9, 3RD TO LEFT). This is confirmed by the line profiles through the images (Fig. 8 and Fig. 9, RIGHT). With 3D acquisition trajectories such as saddle, there is no single ray that looks at the phantom from exactly the same vantage, resulting in more complete sampling and removal of overlapping structures. Although more lesions can be clearly seen when the cone beam is flat near the top of the breast (i.e. -10° tilt), complex 3D trajectories allow for less distortion and more complete sampling (Fig. 10).

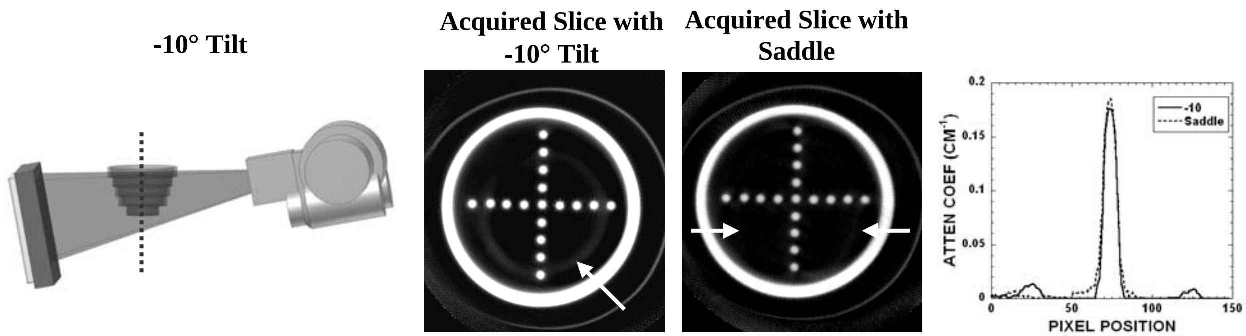

Figure 8: (LEFT) 3D CAD drawing of the setup of the -10° tilted orbit with a black dashed line indicating the vertical axis of rotation. (2ND TO LEFT) Reconstructed slice of the third smallest spherical cross phantom obtained with -10° tilted orbit. Arrow illustrates of an overlapped region (shown in arrow) due to sampling insufficiency acquired with a fixed polar tilt. (3RD TO LEFT) Reconstructed slice of the same phantom acquired with the saddle trajectory. No overlapped region is seen. (RIGHT) Line profile (shown in arrow on the Saddle slice) shows that there is some artifact in the slice acquired with the -10° tilt.

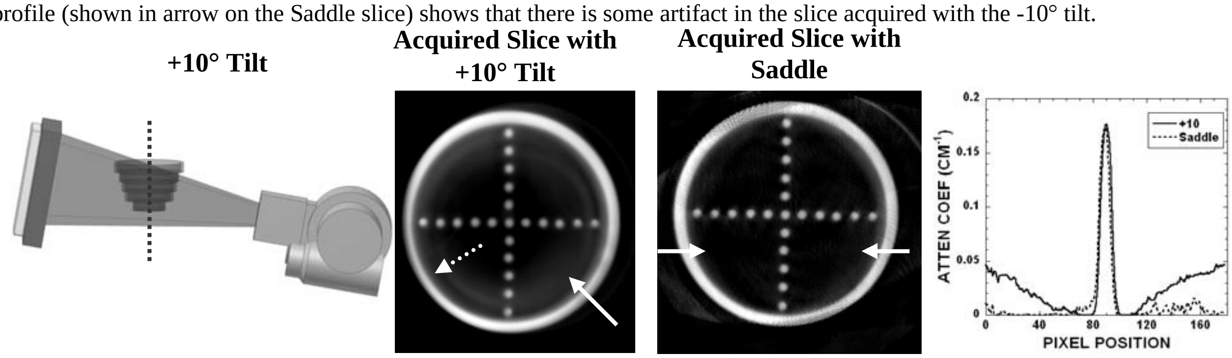

Figure 9: (LEFT) 3D CAD drawing of the setup of the +10° tilted orbit with a black dashed line indicating the vertical axis of rotation. (2ND TO LEFT) Reconstructed slice of the second largest spherical cross phantom obtained with -10° tilted orbit. Solid arrow illustrates an overlapped region due to sampling insufficiency acquired with a fixed polar tilt. Dotted arrow illustrates the geometric distortion of the acrylic frame. (3RD TO LEFT) Reconstructed slice of the same phantom acquired with the saddle trajectory. No overlapped region or geometric distortion is seen. (RIGHT) Line profile (shown in arrow on the Saddle slice) shows that there is some artifact in the slice acquired with +10° tilt.

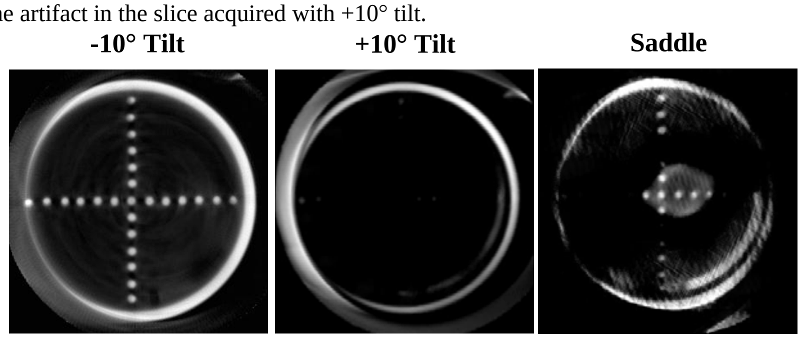

Figure 10: Reconstructed slice of the top spherical cross phantom acquired at (LEFT) -10°, (MIDDLE) +10° tilt, and (RIGHT) Saddle trajectory. As shown in the 3D CAD drawing, the top plane at the -10° tilt is more uniformly sampled. Even though more lesions are seen at the -10° tilt, 3D complex trajectories have less distortion and more complete sampling in the rest of the reconstruction volume.

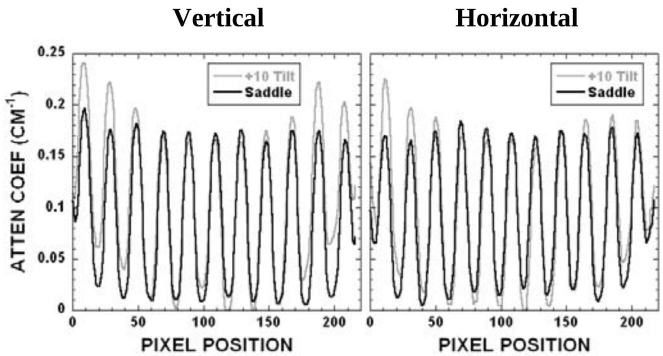

Figure 11: (LEFT) Vertical and (RIGHT) horizontal profiles over lesions of the second largest spherical cross phantom obtained with +10° tilt and saddle shown in Fig. 9. There is a cupping artifact seen with the fixed tilt orbit by observing the intensities from the edge towards the center, which could be mistaken as due to scatter. This is missing from the saddle acquired data due to its more sufficient sampling throughout the imaged volume.

Profiles drawn over the lesions of the second largest spherical cross phantom shown in Fig. 9 are shown in Fig. 11. Vertical and horizontal profiles show that the insufficient sampling from a fixed tilt orbit results in a cupping-type artifact, which could be mistaken for scatter or beam hardening. Since the spheres are virtually suspended in air on a thin plastic sheet, scatter is minimal in this experimental setup. Thus, any scatter correction applied to this region may "flatten" the response across the image, but would incorrectly account for the measured scatter response, which is really due to an artifact from insufficient sampling with a fixed cone beam source tilt.

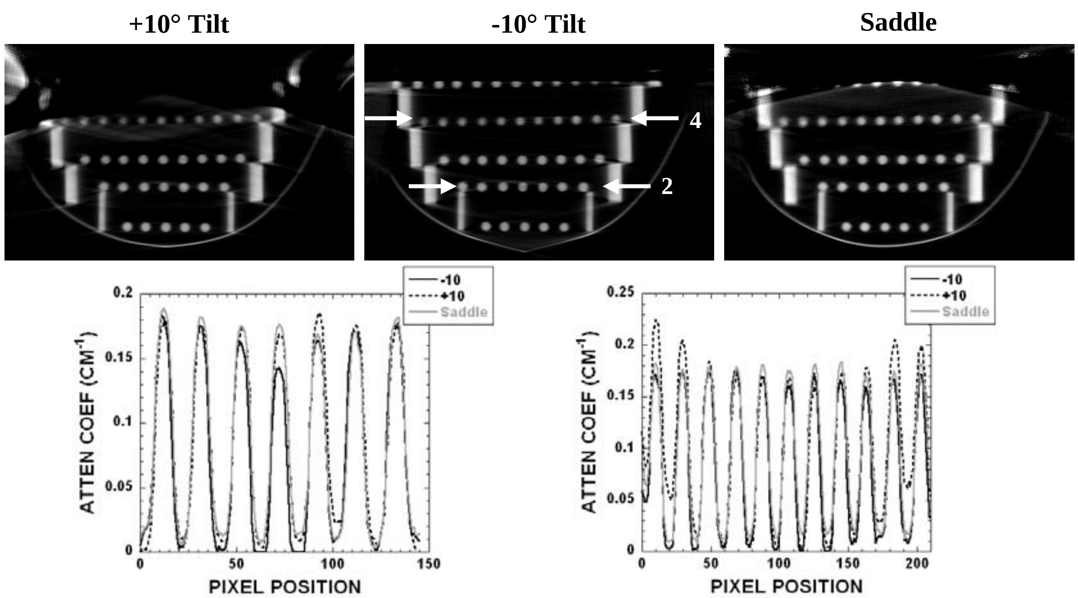

Figure 12: (TOP) Sagittal reconstructed slices of the spherical cross phantoms acquired with indicated trajectories. (BOTTOM) Profiles drawn through spherical cross phantom (BOTTOM LEFT) at level 2 (indicated in TOP MIDDLE image) and (BOTTOM RIGHT) at level 4. -10° tilt shows greater peak uniformity at the 4th level sphere phantom, while +10° tilt shows more uniformity at the 2nd level of the phantom. Saddle trajectory shows peak height uniformity along both cross phantoms.

Effects of sampling insufficieny were also seen in the reoriented sagittal slices of the data (Fig. 12). When the system is at a -10° tilt, there is better sampling at the top of the reconstructed volume rather than the bottom as seen by the uniformity of the peak heights of the profiles across the FOV. This is reversed for the +10° tilt, which again shows a similar cupping artifact as illustrated earlier in Fig. 11, which plane was located at an extreme of the cone beam. However, while the particular image shows artifacts at the top with a saddle trajectory, there is uniformity along the entire reconstructed volume for the indicated spheres.

In order to assess whether these phenomenon are visible in more solid objects, the breast containing the spheres was uniformly filled with mineral oil. Due to the physical distortion of the breast phantom when filling it with oil (i.e. the added weight), only the four smallest circular phantoms fit in the breast shell. Fig. 13 shows the reconstructed slices of the 3rd smallest circular phantom in the breast filled with oil measured with different trajectories. Horizontal profiles were drawn over the lesions (Fig. 14). Just as in the experiments in air, the negative tilt orbits showed more uniform sampling since this layer of the phantom was located closer to the flat part of the cone beam.

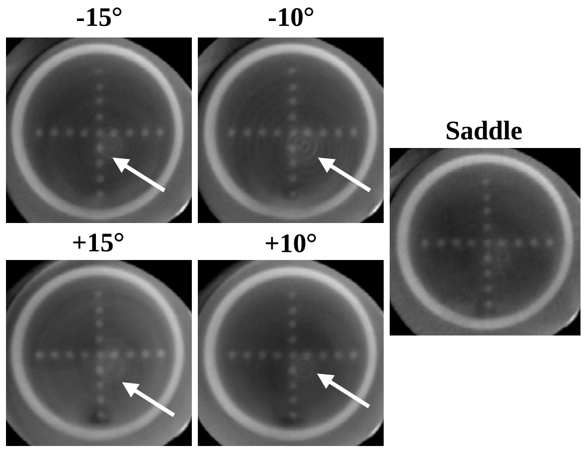

Figure 13: Reconstructed slices of spherical cross phantom in oil acquired at various acquisition trajectories as indicated. Images acquired with a stationary polar tilted, circular orbit had a circular ring (indicated by arrow) in some of the reconstructed slices. However, in the same slice for the saddle trajectory, there is no circular ring apparent.

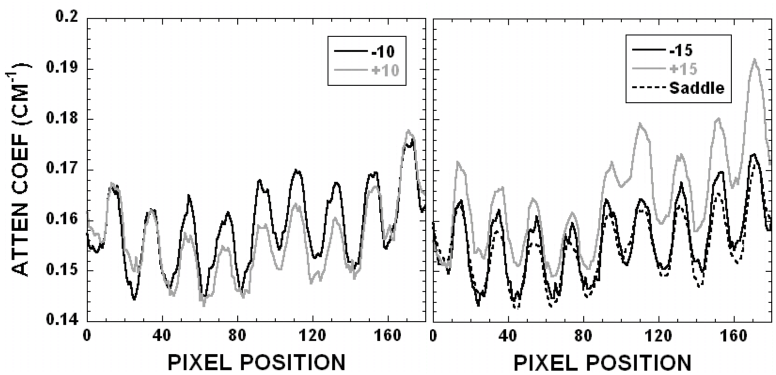

Figure 14: Horizontal profiles of (LEFT) ±10° and (RIGHT) ±15° tilts and saddle at the 3rd ring level from the nipple. Negative tilts and 3D complex trajectories show more uniform sampling.

When closely observing the reconstructed images for all trajectories, a circular ring appears in the reconstructed slices, except for the saddle trajectory (Fig. 13). Typically, such a circular ring in reconstructed images is caused by a bad pixel or series of them in the detector. We believe this is the case here for the fixed tilt orbits. However, the advantage of using a 3D complex trajectory such as saddle is that the same bad pixel does not always view the object from the same vantage, in contrast to simple circular orbits. Because of this, reconstructed images acquired with the saddle trajectory tend to not have these artifacts.

FWHM values were calculated for the outer lesions in the top sphere phantom (level 4). Some of these values are shown below (Fig. 15). Similar to the case shown in air, it is seen that the -10° has a smaller FWHM values (less spread) than rest of the orbit. At this slice, this specific orbit has more complete sampling since the rays are more towards the flat part of the cone beam as shown in the 3D CAD drawing in Fig. 8.

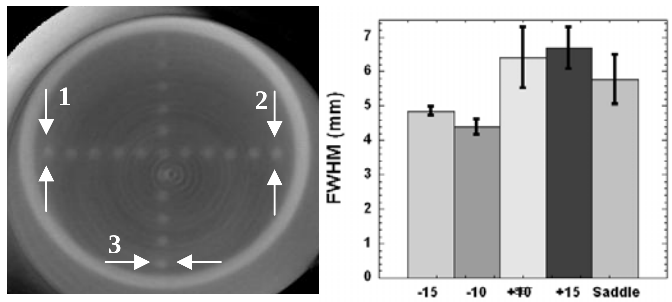

Figure 15: (LEFT) Reconstructed slices of the top spherical cross phantom in oil acquired at -10° acquisition tilt. FWHM values were determined over the lesions specified by the numbered arrows. (RIGHT) Mean FWHM values (in mm) over the lesions in the top circular phantom in oil. Standard deviation is shown in solid vertical bars.

4. CONCLUSIONS

Imaging with a dedicated dual-modality breast imaging tomographic system may help to improve identification and localization of lesions that is crucial for patient screening, diagnostics and therapeutic monitoring. In this work, we have demonstrated a prototype SPECT-CmT system that can provide volumetric fully-3D registered and fused breast images. This system can image an entire breast close to the chest wall to facilitate the detection and biopsy of small tumors without breast compression. This system has common emission (SPECT) and transmission (cone beam CT) FOVs that intersect each other, as opposed to being either on separate systems or linearly juxtaposed on separate gantries.

The CT component of the hybrid assembly was characterized for various system orientations and acquisition trajectories. Results of MTF evaluation in 3D show that there is little difference in the measured MTF throughout the volume regardless of the particular imaging geometry used. However, this may be due to the fact that an iterative algorithm is used to reconstruct the high contrast thin-line source data, after blurring the projection data by binning to 4x4 pixels.

Imaging results of plastic spheres suspended throughout the 3D breast volume and acquired using stationary polar tilted simple circular orbits demonstrated geometric distortions and reconstruction inaccuracies that manifest themselves as cupping artifacts. Slight blur was seen around the spheres near the edges of the FOV. Additional blur was progressively observed away from the flat plane of the cone beam, which had the more complete sampling using simple circular orbits and tilted source-detector angles. These artifacts are in addition to but are distinct from any scatter or beam hardening induced cupping artifacts, indicating that simple scatter correction algorithms present in some systems may overestimate the component, since the cupping artifact is a threefold feature in undersampled cone beam data. Cupping artifacts are thought to be comprised of: scatter, beam hardening and sampling. The latter two are intrinsically corrected for in our independent dedicated breast CT system since we use a quasi-monochromatic beam which virtually eliminates beam hardening[10,16] and complex 3D sampling strategies to acquire more completely sampled cone beam projections of the breast as described previously[11,12] and in this paper.

Currently in our prototype dual-modality system, the CmT component has a stationary tilt. Results indicate that by having the cone beam flat near the top of the breast allows for more complete sampling near the chest wall and more lesions can be clearly seen than for a completely sampled complex 3D trajectory. The drawback is that there are overlapping structures, geometric distortion, and incomplete sampling in the rest of the reconstruction volume. Therefore, for more distortion free images, use of complex 3D trajectories in imaging procedures having more complete sampling is suggested. The volume limitation issue of complex sampling may be ameliorated by lowering the object farther into the FOV, provided it is possible to do so. Specific design of a patient support apparatus is underway in our lab to try to accommodate this[15].

ACKNOWLEDGEMENTS

This work was supported by NIH R01-CA096821, and in part by DOD W81XWH-06-1-0791, and DOD W81XWH-05-1-0280.

REFERENCES

[1] P. D. Shreve, "Adding structure to function," J Nucl Med **41**, 1380-1382 (2000).
[2] O. Israel, Z. Keidar, G. Iosilevsky, et al., "The fusion of anatomic and physiologic imaging in the management of patients with cancer," Semin Nucl Med **31**, 191-205 (2001).
[3] T. F. Hany, H. C. Steinert, G. W. Goenes, A. Buck and G. K. vonSchulthess, "Improvement of diagnostic accuracy of PET imaging using an in-line PET-CT system - initial results," Radiology **225**, 575-581 (2002).
[4] B. H. Hasegawa, K. H. Wong, K. Iwata, et al., "Dual-modality imaging of cancer with SPECT/CT," Tech. Canc. Res. Treatment **1**, 449-458 (2002).
[5] O. Schillaci and G. Simonetti, "Fusion imaging in nuclear medicine: applications of dual-modality systems in oncology," Cancer Biother Radiopharm **19**, 1-10 (2004).
[6] P. Madhav, D. J. Crotty, R. L. McKinley and M. P. Tornai, "Initial development of a dual-modality SPECT-CT system for dedicated mammotomography," 2006 IEEE Nucl Sci Symp & Med Imag Conf (2006).
[7] D. J. Crotty, C. N. Brzymialkiewicz, R. L. McKinley and M. P. Tornai, "Optimizing orientation of SPECT and CT detectors through quantification of cross contamination in a dual modality mammotomography system," 2005 IEEE Nucl Sci Symp & Med Imag Conf **3**, 1672-1676 (2005).
[8] D. J. Crotty, C. N. Brzymialkiewicz, R. L. McKinley and M. P. Tornai, "Investigation of emission contamination in the transmission image of a dual modality computed mammotomography system," 2006 Proc SPIE: Phys Med Imag **6142**, 664-674 (2006).
[9] C. N. Brzymialkiewicz, M. P. Tornai, R. L. McKinley, S. J. Cutler and J. E. Bowsher, "Performance for dedicated emission mammotomography for various breast shapes and sizes," Phys Med Biol **51**, 5051-5064 (2006).
[10] M. P. Tornai, R. L. McKinley, C. N. Brzymialkiewicz, et al., "Design and development of a fully-3D dedicated x-ray computed mammotomography system," 2005 Proc SPIE: Phys Med Imag **5745**, 189-197 (2005).
[11] R. L. McKinley, M. P. Tornai, C. N. Brzymialkiewicz, et al., "Analysis of a novel offset cone-beam transmission imaging system geometry for accommodating various breast sizes," Medica Physica **XXI**, 46-53 (2006).
[12] R. L. McKinley, C. N. Brzymialkiewicz, P. Madhav and M. P. Tornai, "Investigation of cone-beam acquisitions implemented using a novel dedicated mammotomography system with unique arbitrary orbit capability," 2005 Proc SPIE: Phys Med Imag **5745**, 609-617 (2005).
[13] C. N. Brzymialkiewicz, M. P. Tornai, R. L. McKinley and J. E. Bowsher, "Evaluation of fully 3D emission mammotomography with a compact cadmium zinc telluride detector," IEEE Trans. Med. Imag. **24**, 868-877 (2005).
[14] C. N. Brzymialkiewicz, R. L. McKinley and M. P. Tornai, "Towards patient imaging with dedicated emission mammotomography," 2005 IEEE Nucl Sci Symp & Med Imag Conf **3**, 1519-1523 (2005).
[15] D. J. Crotty, P. Madhav, R. L. McKinley and M. P. Tornai, "Patient bed design for an integrated SPECT-CT dedicated mammotomography system," Presented at the *2006 Workshop on the Nuclear Radiology of Breast Cancer*, San Diego, CA, 4-5 Nov. 2006, and published in *2006 IEEE Nuclear Science Symposium & Medical Imaging Conference Record*.
[16] R. L. McKinley, M. P. Tornai, E. Samei and M. L. Bradshaw, "Initial study of quasi-monochromatic beam performance for x-ray computed mammotomography," IEEE Trans. Nucl. Sci. **52**, 1243-1250 (2005).
[17] P. Madhav, R. L. McKinley, E. Samei, J. E. Bowsher and M. P. Tornai, "A novel method to characterize the MTF in 3D for computed mammotomography," 2006 SPIE Med Imag Conf **6142**, (2006).
[18] H. K. Tuy, "An inversion formula for cone-beam reconstruction," SIAM J. Appl. Math. **43**, 546-552 (1983).

APPENDIX C: 2008 IEEE NUCLEAR SCIENCE AND MEDICAL IMAGING CONFERENCE RECORD

Comparison of Reduced Angle and Fully 3D Acquisition Sequencing and Trajectories for Dual-Modality Mammotomography

Spencer J. Cutler, *Member, IEEE*, Priti Madhav, *Member, IEEE*, Kristy L. Perez, *Member, IEEE*, Dominic J. Crotty, *Member, IEEE*, Martin P. Tornai, *Senior Member, IEEE*

***Abstract*– A dual-modality SPECT-CT system for dedicated 3D breast cancer imaging is under development. Independent dedicated SPECT and CT imaging systems have been integrated onto a single gantry for uncompressed breast imaging. This study examines challenges and tradeoffs involved in integrating the acquisition procedures of two independent imaging systems into a single imaging protocol. The physical limitation of the rotating CT tube beneath the custom patient bed currently provides only a 294 degree scan with the bed low enough for the breast to be in the cone-beam CT field-of-view. The directly coupled SPECT system is therefore also limited if the scans are to be taken simultaneously or in an interleaved fashion. Thus, geometric phantoms are imaged to characterize image degradations due to reduced projection angles for both modalities. Two different acquisitions were performed: one with the central ray of the CT cone-beam aligned with the system's center of rotation and one offset from the center of rotation by 5cm. Various sized activity-filled lesions in an anthropomorphic breast phantom were imaged, first with uniform aqueous background activity and then with added acrylic pieces to simulate a non-uniform background. Interleaving the SPECT and CT acquisitions into a single scan was also investigated. Iterative reconstruction algorithms are used to reconstruct the data, and the SPECT and CT images are co-registered. Both the cold rod and breast data indicate that removing 75^{o} of SPECT azimuthal data does not significantly reduce image quality. CT images were also minimally affected if the cone-beam is centrally aligned with the center of rotation, but degraded with the laterally offset cone–beam setup. In the course of these experiments, the patient bed was reconfigured with a larger central hole covered with flexible neoprene, gaining the ability to rotate completely around the breast and dramatically improving CT projection views through the chest wall.**

I. INTRODUCTION

INDEPENDENT SPECT and x-ray CT subsystems developed in our lab have been integrated into a single system for pendant uncompressed, fully-3D multimodality breast imaging, providing co-registered volumetric anatomical and functional information [1]. A custom-designed patient bed was also developed with the goal of maximizing patient comfort while imaging close to the chest wall [2]. This study examines challenges and tradeoffs involved in integrating the acquisition procedures of two independent imaging systems into a single imaging protocol.

The benefits of simultaneous or interleaved SPECT-CT imaging include potentially shorter overall imaging times, simpler inherent image registration, and more straightforward SPECT attenuation correction using the corresponding CT data. Consecutive scans benefit from improved and more uniform 3D SPECT resolution and sampling. Emission contamination of the CT images can also be avoided by acquiring the CT scan prior to radionuclide injection of the patient [3].

Reduced or limited angle tomography has been investigated for both emission and transmission breast imaging [4-9]. These studies usually involve limited circular imaging trajectories of less than 180 degrees. Our objective is to qualitatively examine the tradeoffs of removing a much smaller portion of the full 360 degree azimuthal imaging arc. The SPECT component of our system also introduces the question of how reduced angle tomography affects complex 3D imaging trajectories [10, 11].

II. MATERIALS & METHODS

Specifics and materials of the individual subsystems, combined hybrid SPECT-CT system, as well as the patient bed have been detailed previously [1, 2, 12, 13].

The physical limitation of the rotating CT tube beneath the custom patient bed, combined with the dead edge at the top of the CT detector, currently prevents a full 360 degree dual-modality scan with the bed low enough for the breast to be fully in the cone-beam CT field-of-view (FOV). To increase the volume of the breast in the FOV, the bed was lowered and projection images were acquired at a reduced number of angles (~294 degrees) about the breast, avoiding the head rest of the patient (Fig. 1). The directly coupled SPECT system is therefore also limited in motion if the scans are taken simultaneously in the common FOV. Alternatively, following a reduced angle CT scan, a separate SPECT scan can be made by fixing the SPECT system center of rotation (COR) higher

Manuscript received November 23, 2007. This work was supported by the National Cancer Institute of the National Institutes of Health (R01-CA096821) and in part by the Department of Defense Breast Cancer Research Program (W81XWH-06-1-0765 and W81XWH-06-1-0791) and IEEE Student Travel Award.

The authors are with the Department of Radiology at Duke University Medical Center, Durham, NC 27710. S.J. Cutler, P. Madhav, D.J. Crotty, and M.P. Tornai are also with the Department of Biomedical Engineering at Duke University, Durham, NC 27708. K.L. Perez and M.P. Tornai are also with the Medical Physics Graduate program at Duke University Medical Center, Durham, NC 27710 (email:spencer.cutler@duke.edu).

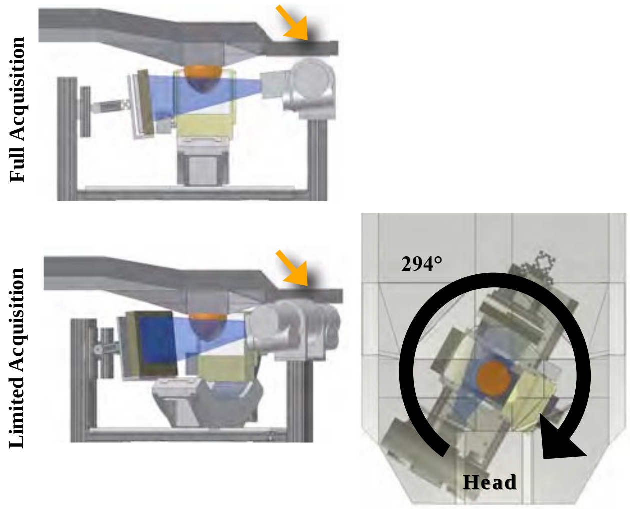

Fig 1: 3D CAD drawings of a (TOP) full and (BOTTOM) limited acquisition setup. The trough for the head (shown by the orange arrow) and physical dimensions of the x-ray tube limit the amount of breast volume in the FOV with a 360º scan, in contrast to a 294° acquisition where the breast can be further dropped into the FOV.

than the CT system and raising the bed to allow a 360^o clearance of the CT tube and detector.

A. Geometric Phantom Study

A mini-cold rod phantom (model ECT/DLX-MP, *Data Spectrum Corp.*, Hillsborough, NC) placed in a 7.7cm inner diameter cylinder was first used to characterize reduced angle tomography for both the SPECT and CT systems. The 2.6cm long rods were arranged in six sectors of equal diameters of 4.7, 3.9, 3.1, 2.3, 1.5, and 1.1mm, on a pitch of twice their diameters. 9.5mCi of ^{99m}Tc in water filled the interstitial spaces. The phantom was suspended vertically with the mini-rods in the center of the camera's field of view and parallel to the camera surface.

Data were acquired on the independent SPECT system using a simple 128 projection vertical-axis-of-rotation (VAOR) orbit over 360^o, acquired for 27 seconds per projection. This yielded a count rate of ~3.5kcounts/sec or approximately 95k counts per projection (in a ±4% energy window). List-mode data from the full 360^o acquisition were then post-processed by removing projections to simulate reduced angle acquisitions of 180^o, 240^o, and 300^o. The list-mode projection data were also truncated such that the total number of counts over the entire acquisition remained the same in an effort to make a time-normalized comparison of the varying reduced angle trajectories. SPECT data were reconstructed using an ordered subsets emission iterative algorithm [14]. Reconstructions were performed using a 2.5mm^3 voxel size on a 150x150x150 grid, using 8 subsets, and 20 iterations.

With a source-to-image distance (SID) of 55cm, a source-to-center-of-object distance (SOD) of 35cm, and a COR to detector distance of 20cm, CT scans of the cold rod phantom were acquired at a tube potential of 60 kVp using a Ce 100th attenuating value layer (0.0508cm) filter (Z=58, r=6.77g/cm3, K-edge=40.4keV, *Santoku America, Inc.*, Tolleson, AZ) to

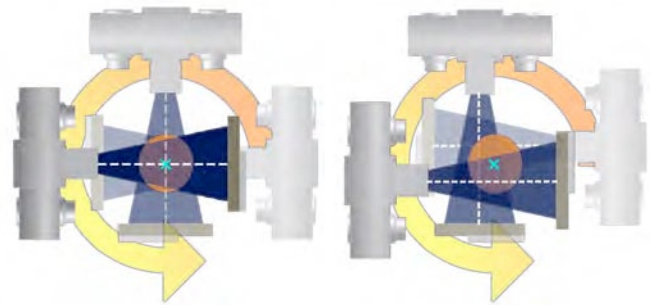

Fig. 2. (LEFT) Schematic illustrating the CT system with central ray of the cone-beam (white dashed line) aligned with the COR (blue x). This setup results in truncation of larger breasts (>15cm in diameter). (RIGHT) Schematic illustrating the advantage of the 5cm offset half-cone-beam used to acquire data for larger breast volumes.

yield a mean energy of ~36keV and FWHM of 15%. Two scans were performed for each set of phantoms: one with the central ray of the cone beam intersecting the axis of rotation (Fig. 2, LEFT), and one with the central ray offset 5cm laterally from the axis of rotation (Fig. 2, RIGHT). The centrally aligned setup results in truncation of larger breasts (>15cm in diameter) and therefore, a 5cm offset cone-beam is currently used in order to acquire data for larger breast volumes [15]. Data were acquired over 360^o in 1.5^o increments with VAOR. Reduced angle CT realizations of 180^o, 240^o, and 300^o were created by removing raw data projections. CT data were reconstructed using an ordered subsets transmission iterative algorithm [16]. Reconstructions were performed on 4x4 pixel binned image data (equaling a 0.508 mm voxel size) on a 350x350x384 reconstruction grid, using 16 subsets, and 10 iterations.

B. Breast Phantom with Homogeneous Background

A 900mL water-filled breast phantom with three lesions (2.7cm, 1.6cm, and 0.8cm outer diameter, with corresponding 2.3mL, 1.0mL, and 0.35mL volumes) were acquired on the SPECT and CT sub-systems. Each lesion was filled with ^{99m}Tc, with an absolute ratio of 20μCi/mL and ~50μL of CT contrast agent, Gastrografin with iodine (I_2). The lesion:background concentration ratio was 10:1. SPECT projections were acquired using a three-lobed sinusoid projected onto a hemisphere (PROJSINE) with polar tilting range (sinusodial amplitude) from 15 to 45° (Fig. 4, BOTTOM) and CT images were acquired using a fixed 6.2° tilt. The SID was increased to 60 cm, a SOD of 38.1 cm, and a COR to detector distance of 22 cm. This resulted in the same magnification of 1.57 for an object at the system's COR as the independent CT system mentioned in the earlier section. Tube potential and filtration remained the same as the previous study, and the CT system retained the 5cm lateral offset. A ±4% energy window symmetric about the 140keV photo peak was used for the all of the SPECT projections in these studies. Total scan time was ~10 minutes. List-mode data from the full 360^o acquisition were again count-normalized between the scans and cropped to create SPECT acquisitions of 180^o, 240^o, and 300^o. Corresponding CT data were also created by removing raw data projections.

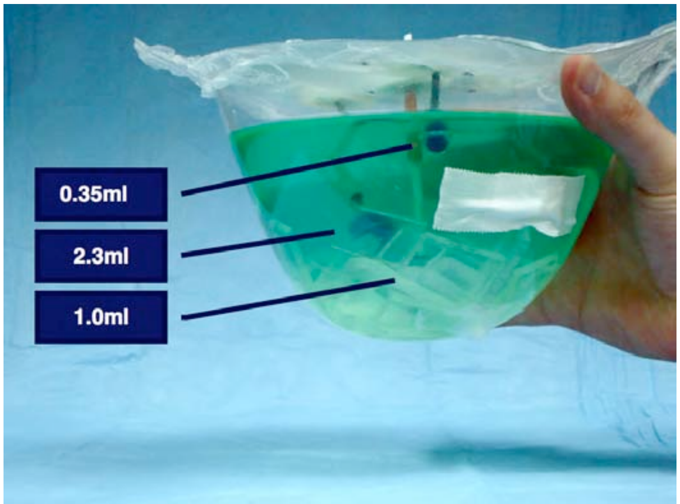

Fig. 3. Breast phantom filled with 900mL of aqueous ^{99m}Tc. Various-sized pieces of acrylic were added to the background to create a heterogeneous background and simulate non-uniform uptake in the SPECT images. Lesion locations and sizes are indicated in the figure.

SPECT reconstruction parameters were set to 3 iterations, 8 subsets, 150x150x150 reconstruction grid, and 2.5mm^3 voxel size. CT reconstruction parameters were set to 5 iterations, 16 subsets, 350x350x384 reconstruction grid, and 508μm^3 voxel size.

C. Breast Phantom with Heterogeneous Background

Small acrylic pieces were added to the same 900mL filled breast to simulate non-uniform uptake in the breast background (Fig. 3). Each lesion was again filled with ^{99m}Tc, with an absolute ratio of 21.8μCi/mL and ~50μL of CT contrast agent (Gastrografin). An activity-filled anthropomorphic heart was also placed above the breast to simulate cardiac uptake and contamination. The lesion:background:heart ratio was 10.8 : 1 : 6.1. Four 6.0mm nylon spheres (*Small Parts, Inc*, Miramar, Fl) were soaked in concentrated aqueous ^{99m}Tc and taped to the exterior surface of the breast phantom to act as fiducial markers for registration purposes.

Two dual modality acquisition sequences were tested with the filled breast phantom: 1) Reduced angle CT and SPECT acquisitions at a single patient bed height, and 2) separate, full 360^o CT and SPECT, each at varying bed heights.

For the first imaging sequence, the patient bed was lowered to the minimal height that the CT tube and detector could still pass beneath the torso of the patient, thereby maximizing the breast volume in the FOV for the rigid bed design. At this height the CT scan is limited to 294^o by the head trough of the bed (Fig 1). CT projections were acquired in 1.5^o increments. Reduced angle SPECT data were then acquired using three trajectories: a tilted-parallel-beam with 45° polar tilt (TPB45), a "Saddle" orbit, and a 3.5-lobed PROJSINE (Fig. 4, CENTER COLUMN). With the bed at minimal position optimized for the reduced angle CT scan, the SPECT polar tilting is limited to a range from 30° to 45°. Reduced angle acquisitions were made with 119 projections over 294° with a

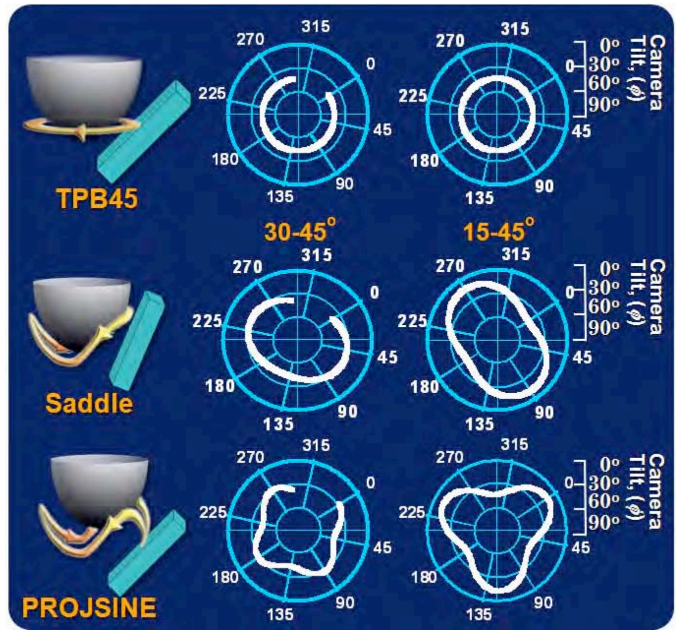

Fig. 4. SPECT acquisition trajectories for the heterogeneous breast phantom studies. Left column shows a 3D illustration of the camera motion. Polar camera tilt as a function of the azimuthal angle is shown for (CENTER COLUMN) reduced angle orbits and (RIGHT COLUMN) full 360^o scans.

total scan time of ~10 minutes per acquisition. Subsequent scans were increased to account for decay.

In the second imaging sequence, the patient bed was raised a few centimeters to allow the tube to rotate fully underneath the head of the patient and CT data were acquired over the full 360^o in 1.5^o increments. The patient bed was then raised again to allow optimal placement of for acquisition of full 360^o TPB45, Saddle, and PROJSINE SPECT scans (Fig. 4, RIGHT COLUMN). Orbits were acquired with 128 projections over 360^o and the total scan time was ~10 minutes.

All other system and reconstruction parameters remained the same as above. SPECT and CT image sets were registered

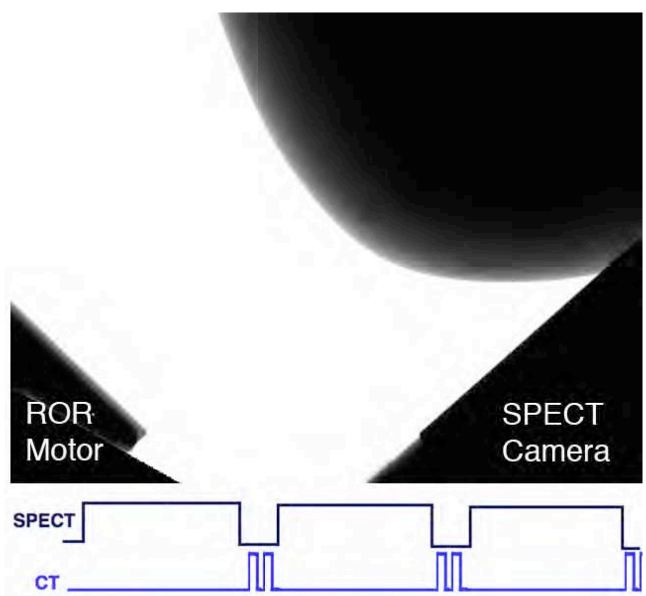

Fig. 5. (TOP) Sample CT projection and (BOTTOM) timing scheme of the interleaved CT scan.

and fused using open source *AMIDE* software [17, 18].

D. *Interleaved SPECT-CT*

Interleaving the SPECT and CT acquisitions into a single scan was also investigated. The acquisition software was modified such that two rapid CT projections were taken between every five-second SPECT acquisition (Fig. 5). Thus the 3-lobed PROJSINE SPECT orbit was sampled in 3^{o} increments while the CT sampled in 1.5^{o} increments over the 360^{o} scan. Because the SPECT camera sometimes obscures a slight corner of the breast in the CT projections, ~2cm was cropped from either side of projection data, effectively removing the corner where acquired data was obscured as previously described. Both uncropped and cropped data were reconstructed using previously described methods.

E. *Modified Patient Bed*

A novel concept included in the patient bed was to design the rigid inner octagonal section of the bed to be removable [2]. This center was removed and replaced with a flexible sheet of neoprene layered leaded apron. The weight of the patient naturally protrudes more of her breast into the FOV and the flexible neoprene increases patient comfort by creating a cushioned hammock. Full 360^{o} dual modality SPECT and CT scans of the same 900mL breast with heterogeneous background were repeated. Lesion-to-background concentration ratios were approximately 10:1. Reconstruction parameters were consistent with earlier parameters, and the reconstructed volumes were fused using *AMIDE*.

III. Results & Discussion

A. *Geometric Phantom Study*

Reconstructed CT slices of the mini-cold rod data where the central ray was aligned with the COR show minimal distortion even with 180^{o} of projection data removed (Fig. 6). The smallest sector of rods (1.1mm) is still resolvable with minor cone-beam sampling artifacts beginning to appear on the left edge. Data insufficiency artifacts from the missing projections are much more visually pronounced with the central ray laterally offset 5cm from the COR (Fig. 7). Regions not seen from all 360^{o} become radially blurred.

For the reconstructed SPECT data, resolution is distance dependant. Even though the cold rods are theoretically fully sampled with 180º of rotation, objects far from the camera will encounter degraded resolution. Hence a 360^{o} scan will improve the image resolution. This is qualitatively seen in the SPECT mini-cold rod reconstructions (Fig. 8). The full 360^{o} images have the highest contrast-resolution. Resolution near the edge of the phantom progressively degrades with decreased angular sampling on that side, as seen in the profiles through the largest 4.7mm rods.

B. *Breast Phantom with Homogeneous Background*

Resolution degradation is not as immediately apparent in the profiles drawn across the largest lesion of the 900mL

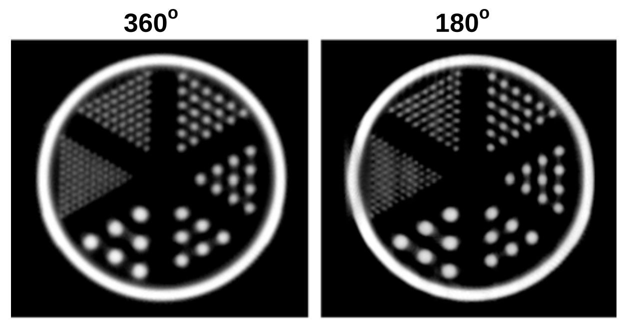

Fig. 6. OSTR iteratively reconstructed CT cold rod data acquired with the central cone-beam ray aligned with the COR. (LEFT) 360^{o} of projection data. (RIGHT) 180^{o} of projection data. Three slices were summed to create these images.

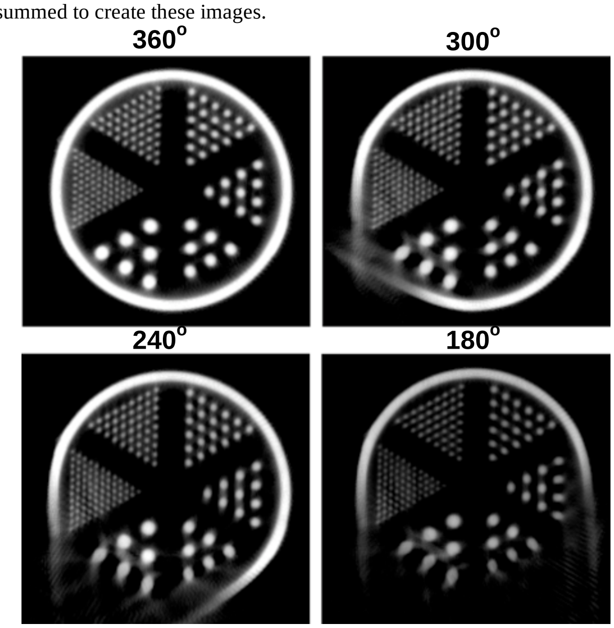

Fig. 7. OSTR Reconstructed CT cold rod data acquired with the central cone-beam ray offset 5cm from the COR. Data insufficiency artifacts become more apparent with decreasing angular sampling.

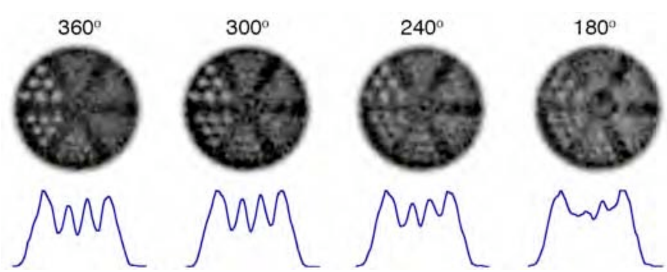

Fig. 8. OSEM reconstructed SPECT mini-cold rod images. Normalized line profiles are shown below, drawn through the largest 4.7mm rods.

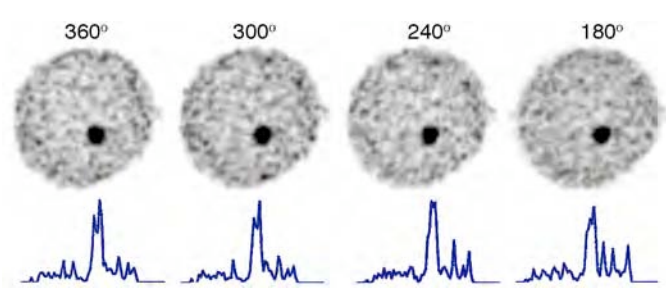

Fig. 9. OSEM reconstructed SPECT breast phantom coronal slices. 2nd iteration shown with 3 summed slices. Normalized line profiles are shown through the 2.3mL lesion.

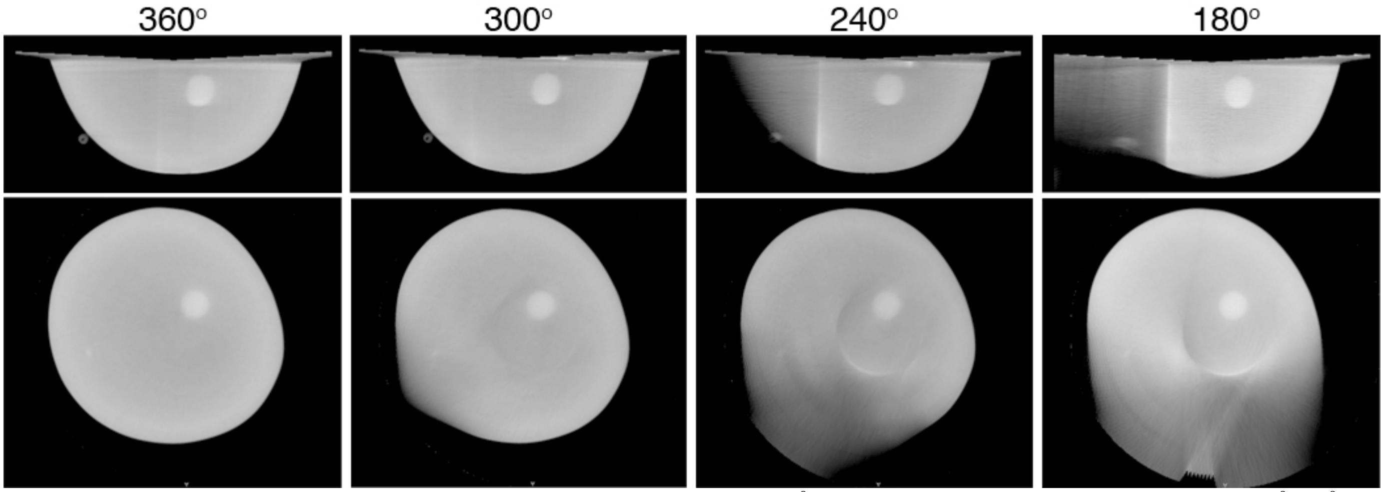

Fig. 10. Reconstructed CT sagittal (TOP) and coronal (BOTTOM) slices. The complete 360^o data are compared with reduced angle scans using 300^o, 240^o, and 180^o of angular sampling. The central cone-beam ray was laterally offset 5cm resulting in truncation artifacts seen in the areas where projection views were not collected.

breast phantom with uniform background (Fig 9). Relative background noise especially on the outer edge of the breast does, however, increase with fewer projections and decreased angular sampling. Both the cold rod and breast data indicate that removing 75^o of SPECT azimuthal data does not significantly reduce image quality.

Reconstructed CT breast images again illustrate artifacts due to incomplete angular sampling (Fig. 10). A distinct loss of attenuation value in the CT reconstructed image on the side where there was no data collected can be measured across the sagittal and coronal slices. In addition, the cylindrical artifacts in the center due to the offset cone-beam became more prominent with decreasing azimuthal acquisition angles.

It is evident from the images of the mini-cold rod and breast phantoms that the lateral offset geometry in our current hybrid system is increasingly penalized when using reduced angle tomography. Disregarding issues of increased scatter, a larger detector with a centrally aligned cone-beam may be a worthwhile solution to avoid truncation of larger breasts for limited angle CT.

C. Breast Phantom with Heterogeneous Background

Truncation artifacts are seen at the bottom of the reconstructed reduced angle SPECT images (Fig. 11). In the current hybrid configuration, the SPECT COR is too near the bottom of the camera face with the bed at the same height as the CT scan. Also because of the limited 30-45^o polar sampling at the low bed height, the air gap between the breast and the heart is less pronounced. Cardiac activity is also more prominent due to more direct views of the heart. In the full 360^o scan, the bed was raised, the polar tilt range of the camera was increased and thus views of the heart were avoided.

In this study the change in polar sampling of the SPECT camera more significantly affected the reconstructed image quality than the reduced azimuthal angular sampling. These results highlight the inherent difficulties in positioning a subject on the bed and the two systems in their current configuration such that the acquisition is simultaneously optimized for both imaging systems. If a universal patient bed height for all of the scans is desired, the SPECT camera needs to be readjusted on the goniometer such that the camera can be positioned to at least 15º polar at the minimum bed height. A single bed height, however, limits the system to a fixed COR and thereby limits the freedom of the SPECT camera. For example, the TPB orbit is more optimal with a lower bed position than the PROJSINE orbit, thus allowing views higher up into the chest and axilla regions.

Fused reconstructed images of the SPECT and CT data illustrate the benefits of combining functional and anatomical information (Fig. 12). The 0.35mL lesion is not more than a suspicious dot in the SPECT images, but its location is verified by the much higher resolution CT images. This lesion, lost in the 360^o scan, also highlights the increased volume seen by the reduced angle scans.

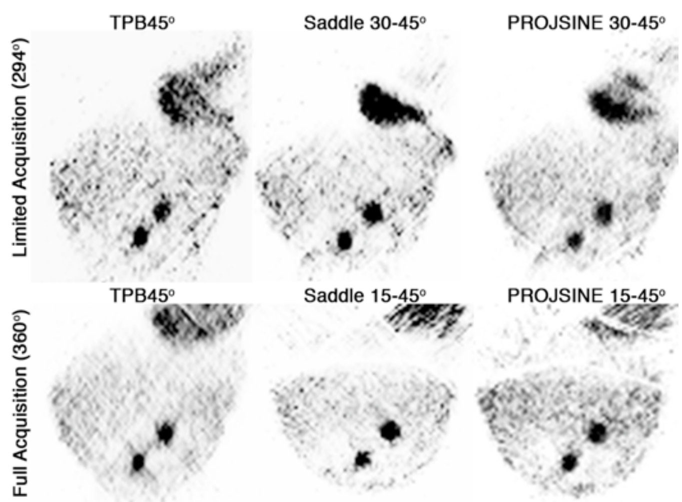

Fig. 11. Sagittal slices of reconstructed SPECT limited angle (TOP) and full 360^o acquisitions (BOTTOM). 2nd iteration is shown with 3 summed slices. 2.3mL lesion is near the center in the breast and 1.0mL lesion is closer to the bottom.

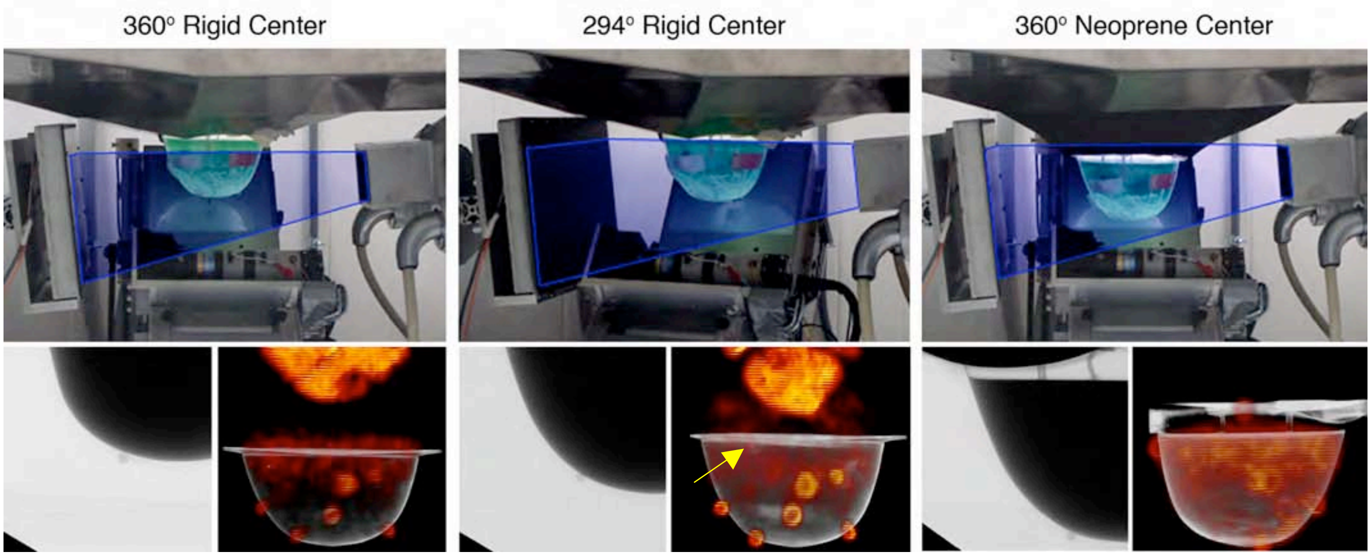

Fig. 12. Breast phantom positioned (TOP LEFT) with bed high enough for 360º clearance, (TOP MIDDLE) with bed lowered to 294º reduced angle scan, and (TOP RIGHT) with flexible center and 360º clearance. Estimated CT cone-beam FOVs are illustrated in blue. Corresponding CT projection data and reconstructed, fused SPECT-CT volume renderings are shown below each system photo. Yellow arrow in bottom center highlights the 3.5mm lesion not seen in the rigid center 360º scan at left. There was no heart activity used in this neoprene study.

D. Interleaved SPECT-CT

The reconstructed images of the interleaved SPECT-CT scan are shown in Fig. 13. As expected there are artifacts near the bottom of the breast due to the close proximity of the SPECT camera. The majority of these artifacts are moved outside of the breast after cropping the projection data 2cm on either side. There is no data loss because of the sampling overlap inherent in the lateral offset geometry. The cropped projection data also reduces the cylindrical offset artifact. No measure of increased x-ray scatter off the SPECT camera or SPECT lesion SNR loss was made in this initial investigation.

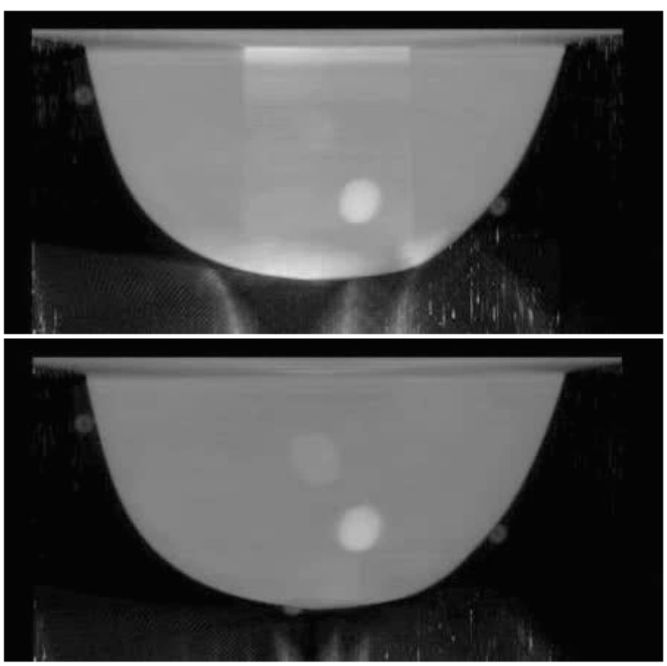

Fig. 13. Volume rendering of iteratively reconstructed CT data acquired in an interleaved fashion with a contouring SPECT scan. Images reconstructed using an (TOP) uncropped and (BOTTOM) cropped

E. Modified Patient Bed

Fig. 12 shows projection views and fused reconstructions of all three patient bed-positioning strategies. The patient bed revised with a larger central hole covered with flexible neoprene center clearly allows a dramatic increase in breast volume in the FOV compared to the rigid steel centerpiece, while now regaining the ability to rotate 360^{o} around the breast. The reconstructed CT data visualizes the entire breast volume, including the air gap above the aqueous activity. With the modified bed, the CT cone-beam could potentially image slightly into the chest wall depending on the positioning of the patient.

IV. Conclusions

Reduced angle tomography can be useful for imaging closer to the chest wall while avoiding physical barriers. Both the mini-cold rod and breast data initially indicate that removing 75^{o} of SPECT azimuthal data will not significantly reduce image quality. Observer based studies are warranted to assess clinical viability. CT images were also minimally affected if the cone-beam is centrally aligned with the COR, but dramatically degraded due to aliasing with the laterally offset cone-beam in our current hybrid system. A larger detector with a centrally aligned cone-beam would be a more ideal solution to avoid truncation of larger breasts for reduced angle CT.

Interleaved SPECT-CT scans can speed up and simplify overall scan time, but limit the positioning freedom of the contoured SPECT orbits. The close proximity of the orbiting SPECT camera created artifacts in the CT images which were reduced by cropping the projection data to reduce the overlap region for shifted-CT, where the SPECT camera obscured CT views of the breast. There may be quantitative losses in an interleaved scan that were not investigated in this initial qualitative study. We opted to use separate sequential CT and SPECT scans because the time saved from the interleaved scan did not justify the artifacts in the CT image and limited positioning freedom of the SPECT scan.

The latest patient bed design with flexible center allows more of the breast into the FOV due to a larger hole in the table and natural extension with the weight of the patient. This permits full 360^o dual modality imaging close to and even slightly into the chest wall. With this revised arrangement, the need to image with reduced angle scans may be alleviated.

ACKNOWLEDGMENT

The authors thank Dr. Randy McKinley for technical assistance and suggestions. Martin P. Tornai is the inventor of this technology, and is named as an inventor on the patent for this technology applied for by Duke. If this technology becomes commercially successful, MPT and Duke could benefit financially.

REFERENCES

[1] P. Madhav, D. J. Crotty, R. L. McKinley, and M. P. Tornai, "Initial Development of a Dual-Modality SPECT-CT System for Dedicated Mammotomography," *2006 IEEE Nucl Sci Symp & Med Imag Conf,* vol. 4, pp. 2382-2386, 2006.

[2] D. J. Crotty, P. Madhav, R. L. McKinley, and M. P. Tornai, "Investigating novel patient bed designs for use in a hybrid dual modality dedicated 3D breast imaging system," *2007 SPIE Med Imag Conf,* vol. 6150, 2007.

[3] D. J. Crotty, C. N. Brzymialkiewicz, R. L. McKinley, and M. P. Tornai, "Investigation of emission contamination in the transmission image of a dual modality computed mammotomography system," *2006 Proc SPIE: Phys Med Imag,* vol. 6142, pp. 664-674, 2006.

[4] J. E. Bowsher, M. P. Tornai, S. D. Metzler, J. Peter, and R. J. Jaszczak, "SPECT breast imaging using more nearly complete orbits and combined pinhole-parallel-beam collimation," *2001 IEEE Nucl Sci Symp & Med Imag Conf,* vol. 3, pp. 1328-1330, 2001.

[5] J. T. Dobbins, 3rd and D. J. Godfrey, "Digital x-ray tomosynthesis: current state of the art and clinical potential," *Phys Med Biol,* vol. 48, pp. R65-106, 2003.

[6] S. P. Poplack, T. D. Tosteson, C. A. Kogel, and H. M. Nagy, "Digital breast tomosynthesis: initial experience in 98 women with abnormal digital screening mammography," *AJR Am J Roentgenol,* vol. 189, pp. 616-623, 2007.

[7] T. Wu, A. Stewart, M. Stanton, T. McCauley, W. Phillips, D. B. Kopans, R. H. Moore, J. W. Eberhard, B. Opsahl-Ong, L. Niklason, and M. B. Williams, "Tomographic mammography using a limited number of low-dose cone-beam projection images," *Med Phys,* vol. 30, pp. 365-380, 2003.

[8] M. P. Tornai, J. E. Bowsher, R. J. Jaszczak, B. C. Pieper, K. L. Greer, P. H. Hardenbergh, and R. E. Coleman, "Mammotomography with pinhole incomplete circular orbit SPECT," *J Nucl Med,* vol. 44, pp. 583-593, 2003.

[9] Y. Zhang, H. P. Chan, B. Sahiner, J. Wei, M. M. Goodsitt, L. M. Hadjiiski, J. Ge, and C. Zhou, "A comparative study of limited-angle cone-beam reconstruction methods for breast tomosynthesis," *Med Phys,* vol. 33, pp. 3781-3795, 2006.

[10] C. N. Brzymialkiewicz, M. P. Tornai, R. L. McKinley, and J. E. Bowsher, "Evaluation of fully 3D emission mammotomography with a compact cadmium zinc telluride detector," *IEEE Trans. Med. Imag.,* vol. 24, pp. 868-877, 2005.

[11] C. N. Brzymialkiewicz, M. P. Tornai, R. L. McKinley, S. J. Cutler, and J. E. Bowsher, "Performance of dedicated emission mammotomography for various breast shapes and sizes," *Phys Med Biol,* vol. 51, pp. 5051-5064, 2006.

[12] D. J. Crotty, P. Madhav, R. L. McKinley, and M. P. Tornai, "Patient bed design for an integrated SPECT-CT dedicated mammotomography system," in *2006 Workshop on the Nuclear Radiology of Breast Cancer,* San Diego, CA, 2006.

[13] R. L. McKinley, C. N. Brzymialkiewicz, P. Madhav, and M. P. Tornai, "Investigation of cone-beam acquisitions implemented using a novel dedicated mammotomography system with unique arbitrary orbit capability," *2005 Proc SPIE: Phys Med Imag,* vol. 5745, pp. 609-617, 2005.

[14] H. M. Hudson and R. S. Larkin, "Accelerated image reconstruction using ordered subsets of projection data," *IEEE Trans. Med. Imag.,* vol. 13, pp. 601-609, 1994.

[15] R. L. McKinley, M. P. Tornai, C. Brzymialkiewicz, P. Madhav, E. Samei, and J. E. Bowsher, "Analysis of a novel offset cone-beam computed mammotomography system geometry for accomodating various breast sizes," *Physica Medica,* vol. 21, pp. 48-55, 2006.

[16] H. Erdogan and J. A. Fessler, "Ordered subsets algorithms for transmission tomography," *Phys Med Biol,* vol. 44, pp. 2835-2851, 1999.

[17] A. M. Loening and S. S. Gambhir, "AMIDE: a free software tool for multimodality medical image analysis," *Mol Imaging,* vol. 2, pp. 131-137, 2003.

[18] D. Stout, "Multimodality image display and analysis using AMIDE," *J Nucl Med,* vol. 48, p. (Supplement 2) 205P, 2007.

APPENDIX D: 2008 IEEE NUCLEAR SCIENCE AND MEDICAL IMAGING CONFERENCE RECORD

Initial Patient Study with Dedicated Dual-Modality SPECT-CT Mammotomography

Priti Madhav, *Member, IEEE*, Spencer J. Cutler, *Member, IEEE*, Kristy L. Perez, *Member, IEEE*, Dominic J. Crotty, *Member, IEEE*, Randolph L. McKinley, *Member, IEEE*, Terence Z. Wong, Martin P. Tornai, *Senior Member, IEEE*

***Abstract*– Dual-modality SPECT-CT dedicated breast imaging offers great promise in the detection/staging of cancer and the monitoring of treatment therapies. The sequential acquisition with emission (nuclear) and transmission (x-ray) 3D imaging systems can aid in localizing the radioactive uptake of a tumor from the emission image by using the anatomical structure from the transmission image as a roadmap. Both independent SPECT and CT subsystems are mounted onto a single gantry that rotates around the vertical axis of a pendant, uncompressed breast. To evaluate the feasibility of this dedicated system, geometric phantoms and breast phantoms using fiducial markers were acquired to study the sampling and resolution properties and demonstrate the fusion of the functional-anatomical images. In addition, a preliminary investigation on the clinical performance of the system was done by imaging two women with confirmed breast cancer: one on the independent SPECT system and the other on the SPECT-CT system. Further patient hybrid imaging studies are in progress. This compact dedicated SPECT-CT system is capable of non-invasively providing complementary functional and anatomical fully-3D activity distribution information of the breast, and has the potential to help further enhance the visual and quantitative information over the independent systems.**

I. Introduction

Breast cancer is one of the most commonly diagnosed cancers among women worldwide and is the second leading cause of cancer death in the United States. However, because of technological advancements in early detection and better treatment options, breast cancer death rates have been dropping since 1990. With early detection, there is less chance of metastasis and the therapeutic treatment of smaller tumors can allow for limited surgery with breast conservation which can help minimize pain, suffering, and increased mortality. Currently, x-ray mammography is the most widely used screening procedure in the U.S., with reported high sensitivity and specificity [1]. However, its limitations including low image contrast, structural overlap, patient discomfort due to breast compression, and imprecise lesion localization have resulted in high false negative rates especially in younger women with denser breasts [2, 3].

These limitations have led to the emergence of fully-3D imaging approaches in magnetic resonance imaging [4], ultrasound [5], nuclear medicine [6, 7], and computed tomography (CT) [8-10] with the goal of improving detection of breast lesions, reducing unnecessary biopsies, and increasing patient comfort. Combined dual-modality systems have also been developed in order to merge complementary information from different modalities to advance patient care and improve diagnostic accuracy [11, 12]. Whole-body SPECT-CT systems have been shown to improve the localization of lymph nodes over planar imaging due to the improved quality of the SPECT images gained by attenuation correction and anatomic landmarks from the CT images [13, 14].

A hybrid scanner has recently been built in our lab for dedicated breast imaging by combining independently developed dedicated breast SPECT and CT technologies [11, 12]. The fully-3D motion capability of the SPECT system allows imaging closer to the breast. Additionally, the quasi-monochromatic nature of the x-ray cone-beam source allows for reduced radiation dose and increased contrast between similar soft tissue attenuation coefficients. The sequential acquisition with emission and transmission systems will aid in the localization of the radioactive metabolic uptake of a tumor with the structural framework of an object.

II. Materials & Methods

The first prototype compact dual-modality system (Fig. 1) was built to image a pendant uncompressed breast. Both SPECT and CT sub-systems are secured to a common rotation stage (model RV350CCHL, *Newport Corp.*, Irvine, CA) to allow an azimuthal rotation of 360° around the vertical axis of the breast. The SPECT sub-system is fixed at 90° relative to the x-ray source-detector axis. A customized patient bed [15-17], positioned over the system, allows a woman to lie prone, suspending a single pendant breast through a hole into the common field of view (FOV) of the hybrid scanner.

A. SPECT Sub-System

The SPECT sub-system uses a compact 16x20cm^2 field of view Cadmium-Zinc-Telluride (CZT) gamma camera (model *LumaGEM* 3200S, *Gamma Medica, Inc.*, Northridge, CA) with discretized crystals, each 2.3x2.3x5mm^3 on a 2.5mm pitch. The measured mean energy resolution of the gamma camera at 140keV is 6.7% FWHM (full-width-half-maximum)

Manuscript received November 23, 2007. This work was supported by NIH R01-CA096821, and in part by DOD W81XWH-06-1-0791 and W81XWH-06-1-0765, Duke University Graduate School, and IEEE Student Travel Award.

P. Madhav, S.J. Cutler, K.L. Perez, D.J. Crotty, R.L. McKinley, T.Z. Wong, and M.P. Tornai are with the Department of Radiology at Duke University Medical Center, Durham, NC 27710. P. Madhav, S.J. Cutler, D.J. Crotty, and M.P. Tornai are also with the Department of Biomedical Engineering at Duke University, Durham, NC 27708. K.L. Perez, T.Z. Wong, and M.P. Tornai are also with the Medical Physics Graduate program at Duke University Medical Center, Durham, NC 27710 (e-mail: priti.madhav@duke.edu).

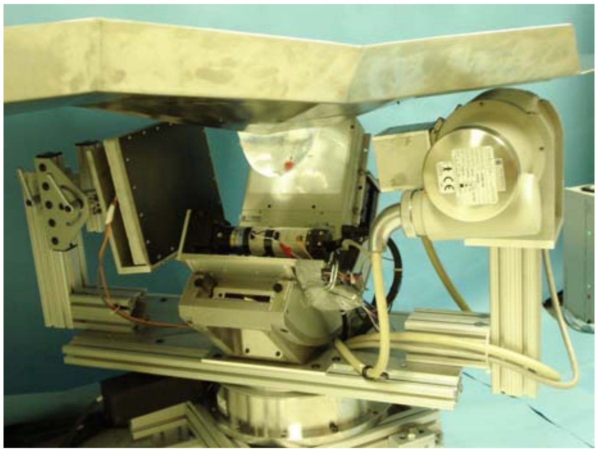

Fig 1: Photograph of the prototype dual-modality dedicated breast imaging tomographic system. The SPECT sub-system (center) is placed orthogonally to the CT tube (right) and digital flat-panel detector (left). The bed is placed above the system with a breast phantom through the center opening in the table. Note that the breast phantom is in the common FOV of each system.

and collimator sensitivity is 37.9 cps/MBq. This system has a parallel-hole collimator with hexagonal holes (1.2mm hole size flat-to-flat (inner diameter), 0.2mm septa, and 25.4mm height). The camera is attached to a laboratory jack (model M-EL120, *Newport Corp.*, Irvine, CA) and a goniometric cradle (model BGM200PE, *Newport Corp.*, Irvine, CA) permitting various radius of rotations (RORs) and 0° to 90° polar tilt angles, respectively. With this flexible gantry, the camera can be positioned anywhere in a hemisphere to facilitate acquiring projection data around a pendant, uncompressed breast [6, 18, 19]. Additionally, the small, high performance dedicated camera, can acquire images close to the breast, thereby minimizing spatial resolution degradation and reducing background contamination from other organs outside the breast volume of interest.

B. CT Sub-System

The CT sub-system consists of a rotating tungsten target cone-beam x-ray source (model Rad-94, 0.4mm focal size, 14° anode angle, *Varian Medical Systems*, Salt Lake City, UT) and CsI(T1)-based amorphous silicon digital x-ray detector (model *Paxscan* 2520, *Varian Medical Systems*, Salt Lake City, UT) with a grid size of 1920x1536 pixels and 127μpixels [10]. The source and detector are secured to a metal plate underneath the SPECT goniometer which is then attached to the azimuthal rotation stage. A filter is inserted into a custom built collimator attached to the x-ray source to produce a quasi-monochromatic x-ray source which can (1) improve the visualization of tissues with very small differences in attenuation coefficients [20]; (2) lower the x-ray dose [21]; and (3) minimize beam hardening [22, 23]. For these studies, a Ce 100^{th} attenuating value layer (0.0508cm) filter (Z=58, ρ=6.77g/cm^3, K-edge=40.4keV, *Santoku America, Inc.*, Tolleson, AZ) was used to yield a mean energy of ~36keV and FWHM of 15%. Source-to-image distance (SID) used was 60cm and source-to-object distance (SOD) was 38.1cm resulting in a magnification of 1.57 for an object located at the system's center of rotation. The central ray of the CT cone-beam is laterally offset 5cm relative to the center of rotation (COR) to completely sample the entire volume of interest [24]. Unlike the SPECT sub-system, the CT sub-system in the combined in the combined scanner is at a fixed 6.2° tilt angle and is restricted to only azimuthal motion.

C. Patient Bed

A customized patient bed, placed over the hybrid device, was built to allow for patient comfort and avoid collision with the imaging system (Fig. 1) [16]. It is comprised of stainless steel, along with a thin lead, neoprene, and polyurethane lining laid on top for patient protection from errant radiation and patient comfort. The lead shielding is used to prevent any contamination from the heart and other organs on the CT images. The bed is angled at the waist in order to support the patient and allow chest protrusion such that the maximal amount of breast volume can fit through the opening in the center which is over the common FOV of both systems. The octagonal trough allows for system rotation underneath it, and a removable insert allows for radiolucent materials to enable imaging up to and through the chest wall.

This bed is attached to a positioning system (model 830-058, *Biodex Medical Systems*, Shirley, NY) which can be displaced in five different directions to allow adjustment for any bowing that might occur due to the weight of the patient and permit the maximal breast volume in the FOV [17]. The head side of the bed is supported to minimize motion of the bed during acquisition.

D. Sampling and Resolution Properties

Using the integrated, prototype hybrid system, images were acquired with a mini-Defrise and mini-cold rod phantoms (*Data Spectrum Crop.* Hillsborough, NC) to study the sampling and resolution properties, respectively. Both phantoms were imaged on the hybrid gantry assembly, but the images were acquired separately: for CT, the phantoms were assembled without any interstitial material (air only), while for SPECT, the phantoms were removed from the FOV, filled with aqueous radioactivity, then scanned.

The mini-Defrise phantom consisted of five 5.0mm discs, spaced 5.0mm apart, in a cylinder with 70mm depth. For the SPECT measurements, 9mCi (333MBq) of aqueous ^{99m}Tc-pertechnetate was distributed between the five acrylic discs creating six "emission discs". In the mini-cold rod phantom, the rods in each of the six sectors have equal diameters of 4.7, 3.9, 3.1, 2.3, 1.5, and 1.1mm, spaced on twice their diameters. For the SPECT measurements, 9.5mCi (351MBq) of aqueous ^{99m}Tc-pertechnetate filled the spaces between the rods. Both phantoms were placed at the COR in the common FOV of the hybrid system. SPECT images were acquired using the vertical axis of rotation (VAOR) orbit. A ±4% energy window symmetric about the 140keV photopeak was used. CT images were acquired with a simple circular orbit at a fixed 6.2° polar tilt.

Reconstructions were done using a ray-driven statistical iterative ordered reconstruction algorithm (ordered subsets expectation maximization (OSEM) for SPECT and ordered subsets transmission (OSTR) for CT). SPECT reconstruction parameters were set to 10 iterations, 8 subsets, 160x160x160 reconstruction grid, and 2.5mm^3 voxel size. CT reconstruction parameters were set to 5 iterations, 16 subsets, 350x350x384 reconstruction grid, and 508μm^3 voxel size. SPECT and CT image sets were registered and fused using an open source *AMIDE* software [25, 26].

E. Breast Phantom

To test image registration and fusion capabilities using non-geometric shapes, images of a 900mL water-filled breast phantom with three lesions (2.7cm, 1.6cm, and 0.8cm diameter) and various sized plastic pieces that simulate non-uniform uptake in the breast background were acquired on the hybrid system. Each lesion was filled with the SPECT radionuclide molecule, aqueous ^{99m}Tc-pertechnetate, (20μCi/mL (0.74MBq/mL) in each lesion) and CT contrast agent (~50μL), Gastrografin with iodine (I_2). The lesion:background radioactive concentration ratio was 10:1. Small and fixed external fiducial markers were used in order to ensure proper registration, be visible and distinguished in both systems, and not interfere with the images. After testing different types of homemade and commercial fiducial markers, four 6.0mm nylon balls (*Small Parts, Inc.* Miami Lakes, FL) soaked in aqueous ^{99m}Tc-pertechnetate were used as markers and taped to the exterior surface of the breast phantom. SPECT images were acquired using a complex acquisition trajectory, three-lobed sinusoid projected onto a hemisphere (PROJSINE) with polar tilting range (sinusodial amplitude) from 15 to 45°. This trajectory for SPECT has been investigated previously [19, 27]. CT images were acquired using a fixed 6.2° tilted circular trajectory. A ±4% energy window symmetric about the 140keV photopeak was used for the SPECT projections.

SPECT reconstruction parameters were set to 2 iterations, 8 subsets, 150x150x150 reconstruction grid, and 2.5mm^3 voxel size. CT reconstruction parameters remained as previously stated. SPECT and CT image sets were registered and fused using *AMIDE*.

F. Patient Study

Two subject volunteers with confirmed breast cancer were imaged under a protocol approved by the Duke University Medical Center institutional review board (IRB). Informed written consent was obtained from both subjects.

The first subject study was imaged with only the independent, dedicated breast SPECT system using an initial prototype, radiolucent bed lined with lead and foam. This bed was modified with a cutout on the side for the patient's left breast. The subject was a 55yr old, post-menopausal, 59kg woman with biopsy confirmed adenocarcinoma (T2N0). She was injected with 17.8mCi (660MBq) of ^{99m}Tc-sestamibi, which has been shown to accumulate selectively in breast malignancies [28], and scanned using a 45º tilted circular trajectory.

The second patient study was done with the hybrid system and the customized patient bed. She was a 45yr old, 93kg patient also with biopsy confirmed breast cancer. Three hours before the hybrid scan, she had received an injection of 29mCi (1073MBq) ^{99m}Tc-methylene diphosphanate (MDP) for a bone scan. While ^{99m}Tc-MDP is used to detect bone metastases, it has much less accumulation in soft tissue tumors, and has been used in early scintimammography studies [29]. However to minimize radiation dose to the patient, the patient was not injected with ^{99m}Tc-sestamibi for the hybrid scan. Four fiducial markers (i.e. nylon balls) were taped to her left breast at 3, 6, 9, and 12 o'clock position. The positioning system of the bed allowed compensation for the bowing of the bed due to the subject's weight. This was done by angling the bed upward and bringing the bed down as far as it could go without hitting the CT tube. In addition, the inner trough of the patient bed was removed to allow more of the breast to protrude into the FOV due to the larger hole in the table and the weight of the patient. The neoprene lining gave additional support and comfort to the subject. After the breast was positioned in the COR of the hybrid system, an 11 minute 360° CT scan was acquired. The patient got up, readjusted

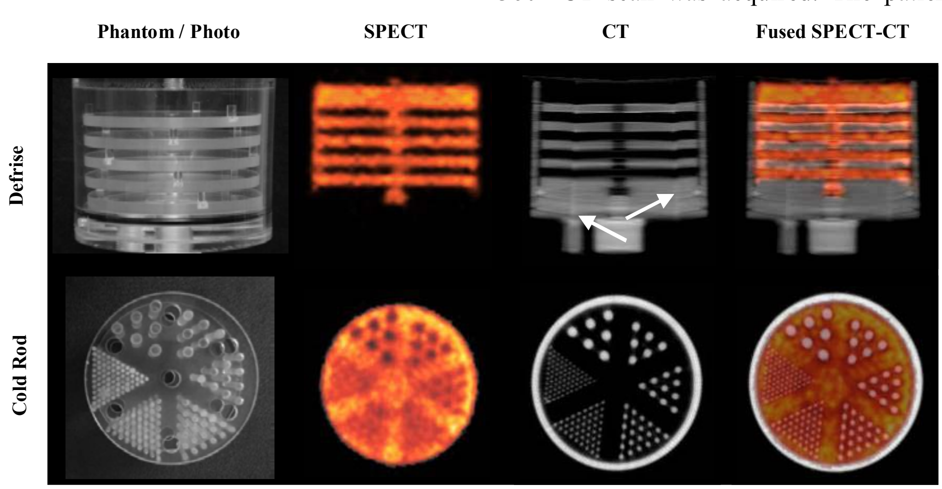

Fig 2: Reconstructed images of the geometric mini-Defrise (TOP ROW) and mini-cold rod (BOTTOM ROW) phantoms were acquired on the hybrid gantry to study the sampling and resolution properties, respectively. CT reconstructed images show slight distortion toward the edges of the mini-Defrise phantom and a circular ring artifact (shown by arrows).

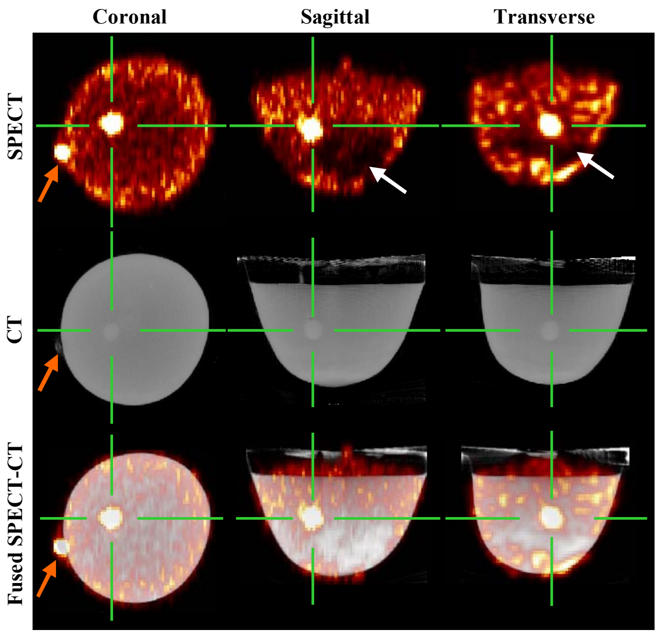

Fig. 3: Reconstructed (TOP) SPECT, (MIDDLE) CT, and (BOTTOM) fused images of a 900mL water-filled breast phantom. The 2.7cm diameter lesion is centered by the green hash marks. Fiducial markers (i.e. nylon balls) were taped to the exterior surface of the breast phantom (orange arrow). Areas with the plastic pieces can be seen as cold spots on the SPECT images (white arrows). The two 3D reconstructed data sets were registered using the fiducial markers.

herself back on the bed, and a 10 minute SPECT scan using a PROJSINE 15-45° trajectory was performed. This procedure was repeated for the right breast, but the SPECT scan was acquired using a fixed 45º tilted circular trajectory.

Both patients were centered using a vertical beam of a positioning laser which was aligned to the COR of the system. Acquisition trajectories were specifically constructed for the SPECT system to contour each individual breast by manually measuring the radius of rotation between the camera and breast at six different azimuthal positions and interpolating other RORs about the breast. Reconstruction parameters were the same as used for the breast phantoms.

III. Results & Discussion

A. *Sampling and Resolution Properties*

The reconstructed SPECT, CT, and fused images of the mini-Defrise phantom are shown in Fig. 2 (TOP). As expected, the SPECT reconstructed images acquired using VAOR has sufficient sampling so all four regions between the discs can be clearly seen without any image distortion. The CT reconstructed images, on the other hand, showed slight distortion toward the edges and a circular ring artifact which possibly results from insufficient sampling due to the tilted and offset geometry, respectively. Corrections for these distortions and artifacts are currently being explored. Despite the sampling insufficiency in the CT image, data was registered using common features in both data sets. It would be more useful to have landmark points, such as external fiducial markers, to obtain the necessary registration accuracy between SPECT and CT images rather than the internal ones used here.

Fig. 2 (BOTTOM) shows the reconstructed images obtained of the mini-cold rod phantom. In the SPECT reconstructed images, the first and second largest sectors of rods (4.7 and 3.9mm, respectively) are clearly distinguishable while the third sector of rods (3.1mm) is nearly distinguishable. In the CT images, all six sectors of rods are clearly resolved. Using the rods in the largest sector as internal fiducial markers, the two image data sets were easily registered.

B. *Breast Phantom Measurements*

Fig. 3 shows the SPECT, CT, and fused reconstructed images. With the help of the fiducial markers, the images from both systems were fused. CT contrast agent was not added to the solution when preparing the fiducial markers since there was enough natural contrast between air and nylon to discriminate them in the projections and reconstructed images (Fig. 3, MIDDLE LEFT). In volumetric 3D space, the SPECT reconstructed images were rotated 90° azimuthally (due to the position of the SPECT sub-system with respect to the CT sub-system) and shifted downward (due to the different bed positions used for SPECT and CT acquisitions). Fiducial markers made it possible to accurately perform these tasks so that the two data sets were aligned as close as possible. As seen in Fig. 3, the location of the plastic pieces are more easily seen in the SPECT reconstructed images as cold spots. However, due to similar attenuation coefficient values between plastic and water, a very narrow window was needed to visualize the plastic pieces in the reconstructed CT slices. This shows the importance of being able to use the anatomical information from CT to guide the localization of suspicious foci seen in the SPECT images.

C. *SPECT Patient Study*

Results of our first SPECT patient study are shown in Fig. 4. There was a clear signal enhancing ~2cm diameter, detailed volume of tracer anterior to the chest wall which corresponded to that seen in the contrast enhanced MRI scan performed earlier in the day. While out of field background activity was minimized due to the use of the radio-opaque pre-prototype bed, streak artifacts and additional enhancing regions that appear in the bottom left of the coronal view and upper left of the transverse view were probably due to the cardiac-hepatic uptake of the radiotracer. Shape distortions were partially due to the incomplete sampling of the tilted parallel beam acquisition trajectory, which are consistent with our previously published results on breast phantoms.

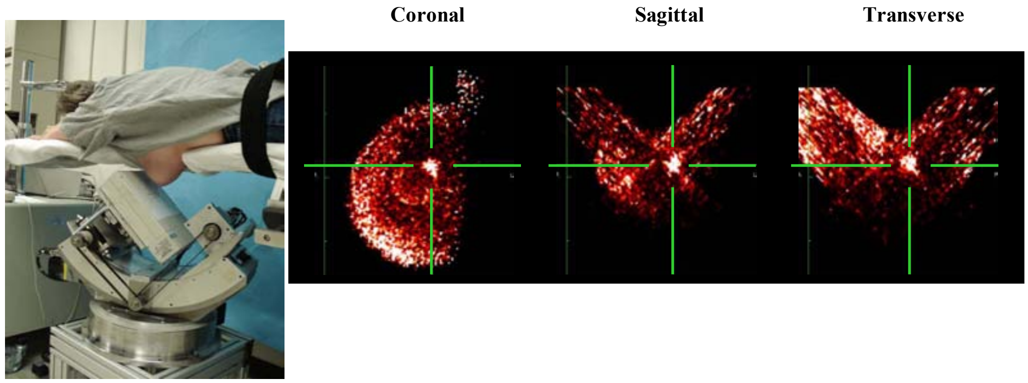

Fig 4: (FAR LEFT) Photograph of the subject on the preprototype bed, suspended over the dedicated breast SPECT system. (RIGHT IMAGES) Reconstructed images of the breast are in coronal, sagittal, and transverse views. Confirmed lesion on the subject's anterior chest wall is indicated at the intersection of the green hash marks

D. Hybrid Patient Study

Fig. 5 shows the results of our first hybrid subject study. Although this patient was confirmed as having breast cancer, no mammogram and/or MRI images of the patient were made available to us to confirm the location of the cancer. Hence, no areas in the SPECT and CT images presented here of this patient's breast can be diagnosed as being a suspected tumor. The SPECT breast scan showed very little uptake of the tracer due to its low accumulation in tumors and soft tissue, and the radioactive decay between the times of the bone and SPECT scan. A couple of different CT slices of the breast are also shown in Fig. 5. The SPECT and CT images shown here were not fused since the fiducial markers moved during the subject's readjustment between scans. By eliminating overlapping tissue, we believe that the CT slices will be able to easily isolate the tumor if breast cancer is present. Similar results are shown for the right breast (Fig. 6). Further patient studies with the hybrid SPECT-CT system are in progress. Results will be compared with mammogram and/or MRI images to confirm that SPECT-CT scans have the potential of breast cancer detection.

IV. CONCLUSION

Advantages of this dedicated dual-modality SPECT-CT breast imaging tomographic system include: (1) volumetric fully-3D whole breast imaging, (2) registration of complementary functional and anatomical images to further enhance quantitative and visual information, (3) SPECT imaging capability nearly completely contouring the breast, axilla, and with views into the chest wall, (4) lower CT x-ray dose to the breast compared to standard dual-view screening mammography, and (5) acquisition of both SPECT and CT images without moving the patient. Complex 3D acquisition trajectories with the SPECT system are useful to avoid physical hindrances, overcome distortions due to inadequate sampling, and allow detection of lesions in the chest wall and axilla that are not visible using simple circular acquisition trajectories. With the offset geometry, the CT system can image a wide range of breast sizes without truncation artifacts, although other imaging artifacts including the circular ring are still present. Methods to remove these imaging artifacts are being studied.

Initial SPECT and hybrid patient studies show promising

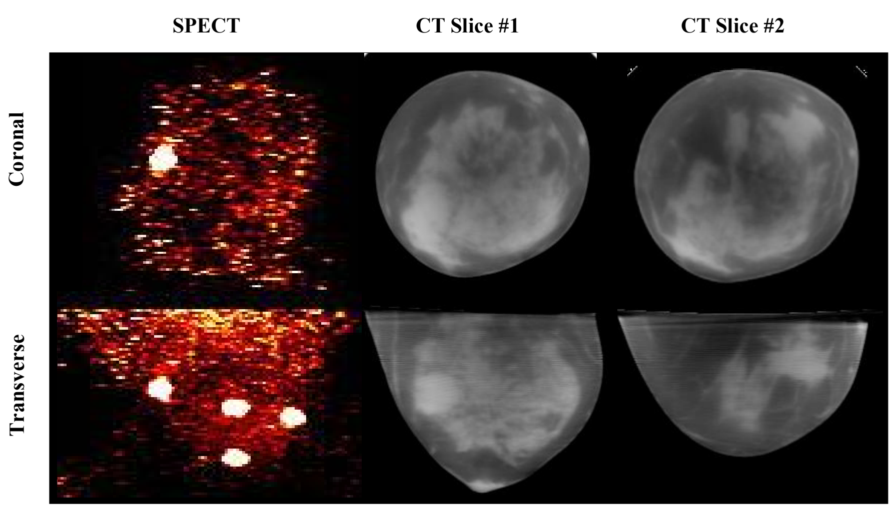

Fig 5: Reconstructed images of the (LEFT) SPECT (shown as a MIP image), (MIDDLE) CT Slice #1, and (RIGHT) CT Slice #2 of the left breast. The bright white spots on the SPECT MIP images are the fiducial markers.

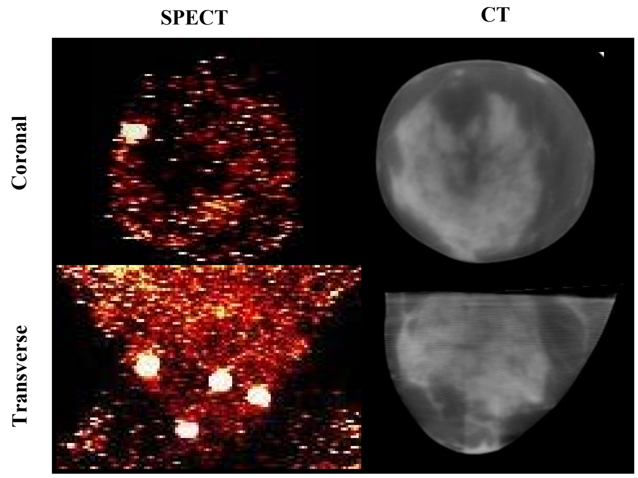

Fig 6: Reconstructed images of the (LEFT) SPECT (shown as a MIP image) and (RIGHT) CT slice of the right breast. The bright white spots on the SPECT MIP images are the fiducial markers.

3D results. Although the SPECT images can see up to and past the chest wall, there is limited visualization of the chest wall in the CT images, which remains an important consideration in planned refinements of the current hybrid system. The physical limitations of the system (i.e. large dead zone of the tube and detector) prevent the breast from being positioned farther into the common FOV; however, the five degrees of freedom in bed movement, replacement of the inner trough with flexible material, and improved patient positioning will hopefully allow the chest wall to be imaged. Patient feedback on the comfort of our patient bed will help us improve future iterations. Further hybrid patient studies are still in progress. We believe that the fused images may provide valuable clinical information for more precise detection, staging, and therapy monitoring of cancerous diseases than independent systems alone.

Acknowledgment

The authors would like to acknowledge several past and ongoing contributions from James Bowsher. Martin Tornai is the inventor of this technology, and is named as an inventor on the patent for this technology applied for by Duke. If this technology becomes commercially successful, Martin Tornai and Duke could benefit financially.

References

[1] J. G. Elmore, K. Armstrong, C. D. Lehman, and S. W. Fletcher, "Screening for breast cancer," *JAMA,* vol. 293, pp. 1245-1256, 2005.

[2] C. A. Swann, D. B. Kopans, K. A. McCarthy, G. White, and D. A. Hall, "Mammographic density and physical assessment of the breast," *Am J Roentgenol,* vol. 148, pp. 525-526, 1987.

[3] V. Jackson, R. Hendrick, S. Feig, and D. Kopans, "Imaging of the radiographically dense breast," *Radiology,* vol. 188, pp. 297-301, 1993.

[4] J. C. Weinreb and G. Newstead, "MR imaging of the breast," *Radiology,* vol. 196, pp. 593-610, 1995.

[5] E. Tohno, D. O. Cosgrove, and J. P. Sloane, *Ultrasound Diagnosis of Breast Diseases*: Churchill Livingstone, 1994.

[6] M. P. Tornai, J. E. Bowsher, C. N. Archer, J. Peter, R. J. Jaszczak, L. R. MacDonald, B. E. Patt, and J.S. Iwanczyk, "A 3D gantry single photon emission tomograph with hemispherical coverage for dedicated breast imaging," *Nucl. Instr. Meth. Phys. Res. A,* vol. 497, pp. 157-167, 2003.

[7] M. B. Williams, A. R. Goode, S. Majewski, D. Steinbach, A. G. Weisenberger, R. F. Wojcik, and F. Farzanpay, "Gamma-ray detectors for breast imaging," *1997 SPIE Med Imag Conf,* vol. 3115, pp. 226-234, 1997.

[8] R. Ning, Y. Yu, D. L. Conover, X. Lu, H. He, Z. Chen, L. Schiffhauer, and J. Cullinan, "Preliminary system characterization of flat-panel-detector-based cone-beam CT for breast imaging," *2004 SPIE Med Imag Conf,* vol. 5368, pp. 292-303, 2004.

[9] J. M. Boone, A. L. C. Kwan, T. R. Nelson, N. Shah, G. Burkett, J. A. Seibert, K. K. Lindfors, and G. Ross, "Performance assessment of a pendant-geometry CT scanner for breast cancer detection," in *2005 SPIE Med Imag Conf*, San Diego, CA, 2005, pp. 319-323.

[10] M. P. Tornai, R. L. McKinley, C. N. Brzymialkiewicz, P. Madhav, S. J. Cutler, D. J. Crotty, J. E. Bowsher, E. Samei, and C. E. Floyd, "Design and development of a fully-3D dedicated x-ray computed mammotomography system," in *2005 SPIE Med Imag Conf*, San Diego, CA, 2005, pp. 189-197.

[11] P. Madhav, D. J. Crotty, R. L. McKinley, and M. P. Tornai, "Initial development of a dual-modality SPECT-CT system for dedicated mammotomography," *2006 IEEE Nucl Sci Symp & Med Imag Conf,* 2006.

[12] M. P. Tornai, P. Madhav, D. J. Crotty, S. J. Cutler, R. L. McKinley, K. Perez, and J. E. Bowsher, "Initial hybrid SPECT-CT system for dedicated fully-3D breast imaging," *J Nucl Med,* vol. 48, p. (Supplement 2) 45P, 2007.

[13] E. Even-Sapir, H. Lerman, G. Lievshitz, A. Khafif, D. M. Fliss, A. Schwartz, E. Gur, Y. Skornick, and S. Schneebaum, "Lymphoscintigraphy for sentinel node mapping using a hybrid SPECT/CT system," *J Nucl Med,* vol. 44, pp. 1413-1320, 2003.

[14] H. Lerman, G. Lievshitz, O. Zak, U. Metser, S. Schneebaum, and E. Even-Sapir, "Improved sentinel node identification by SPECT/CT in overweight patients with breast cancer," *J Nucl Med,* vol. 48, pp. 201-206, 2007.

[15] D. J. Crotty, P. Madhav, R. L. McKinley, and M. P. Tornai, "Patient bed design for an integrated SPECT-CT dedicated mammotomography system," in *2006 Workshop on the Nuclear Radiology of Breast Cancer*, San Diego, CA, 2006.

[16] D. J. Crotty, P. Madhav, R. L. McKinley, and M. P. Tornai, "Investigating novel patient bed designs for use in a hybrid dual modality dedicated 3D breast imaging system," *2007 SPIE Med Imag Conf,* vol. 6150, 2007.

[17] K. L. Perez, P. Madhav, D. J. Crotty, and M. P. Tornai, "Analysis of patient bed positioning in SPECT-CT imaging for dedicated mammotomography," *2007 SPIE Med Imag Conf,* vol. 6510, pp. 371-8, 2007.

[18] C. N. Brzymialkiewicz, R. L. McKinley, and M. P. Tornai, "Towards patient imaging with dedicated emission mammotomography," *2005 IEEE Nucl Sci Symp & Med Imag Conf,* vol. 3, pp. 1519-1523, 23-29 Oct. 2005 2005.

[19] C. N. Brzymialkiewicz, M. P. Tornai, R. L. McKinley, and J. E. Bowsher, "3D data acquisition sampling strategies for dedicated emission mammotomography for various breast sizes," *2005 IEEE Nucl Sci Symp & Med Imag Conf,* vol. 4, pp. 2596-2600, 16-22 Oct. 2004 2004.

[20] P. C. Johns and M. J. Yaffe, "X-ray characterization of normal and neoplastic breast tissues," *Phys. Med. Biol.,* vol. **32**, pp. 675-695, 1987.

[21] R. L. McKinley and M. P. Tornai, "Preliminary investigation of dose for a dedicated mammotomography system," *2006 Proc SPIE: Phys Med Imag,* vol. 6142, pp. 60-70, 11-17 Feb. 2006.

[22] R. L. McKinley, M. P. Tornai, E. Samei, and M. L. Bradshaw, "Simulation study of a quasi-monochromatic beam for x-ray computed mammotomography," *Med. Phys.,* vol. 31, pp. 800-813, 2004.

[23] D. J. Crotty, R. L. McKinley, and M. P. Tornai, "Experimental spectral measurements of heavy K-edge filtered beams for x-ray computed mammotomography," *Phys Med Biol,* vol. 52, pp. 603-616, 2007.

[24] R. L. McKinley, M. P. Tornai, C. N. Brzymialkiewicz, P. Madhav, E. Samei, and J. E. Bowsher, "Analysis of a novel offset cone-beam transmission imaging system geometry for accommodating various breast sizes," *Medica Physica,* vol. XXI, pp. 46-53, 2006.

[25] A. M. Loening and S. S. Gambhir, "AMIDE: a free software tool for multimodality medical image analysis," *Mol. Imaging,* vol. 2, pp. 131-137, 2003.

[26] D. Stout, "Multimodality image display and analysis using AMIDE," *J Nucl Med,* vol. 48, p. (Supplement 2) 205P, 2007.

[27] C. N. Brzymialkiewicz, M. P. Tornai, R. L. McKinley, and J. E. Bowsher, "Evaluation of fully 3D emission mammotomography with a compact cadmium zinc telluride detector," *IEEE Trans. Med. Imag.,* vol. 24, pp. 868-877, 2005.

[28] L. Filippi, A. Pulcini, S. Remediani, E. Masci, A. Redler, F. Scopinaro, and G. D. Vincentis, "Usefuless of scintimammography with Tc-99m MIBI in clinical practice," *Clin Nucl Med,* vol. 31, pp. 761-763, 2006.

[29] S. Piccolo, S. Lastoria, C. Mainolfi, P. Muto, L. Bazziczlupo, and M. Salvatore, "Technetium-99m-Methylene diphosphonate scintimammography to image primary breast cancer," *J Nucl Med,* vol. 36, pp. 718-724, 1995.